JOURNAL OF GEOPHYSICAL RESEARCH, VOL. 103, NO. B1, PAGES 623–650, JANUARY 10, 1998

Forearc structures and tectonic regimes at the oblique subduction zone between the Hikurangi Plateau and the southern Kermadec margin

Jean-Yves Collot

Géosciences Azur, l'Institut Français de Recherche Scientifique pour le Développement en Coopération, Villefranche sur mer, France

Bryan Davy

Institute of Geological and Nuclear Sciences, Wellington, New Zealand

Abstract. The convergent southern Kermadec margin is examined to study the structural development and mechanical parameters of the inner trench slope in response to the oblique subduction of the oceanic Hikurangi Plateau. Swath bathymetric data have been combined with other geophysical data to reveal that the South Kermadec inner trench wall is segmented into distinct upper, middle, and lower margins. The lower margin is a nongrowing, compressionally unstable accretionary wedge that is dissected by transcurrent faults. The wedge has been thinned and narrowed as a result of tectonic erosion. The middle margin is stable by comparison and separated from the lower margin by the 220-km-long Awanui Fault. This fault is a landward dipping, strike-slip, reverse fault. The middle upper margin, including East Cape Ridge (ECR), forms a deforming backstop with a sharp along-strike change in tectonic regime. South of 36°40'S, transpression characterizes the ECR shear zone. North of 36°40'S, the ECR is marked by uplift, by extension, and farther north by subsidence. It is suggested that subsidence and subsequent tectonic erosion of the margin north of 35°50' S, in the wake of Hikurangi Plateau subduction, have broken the link between once continuous segments of the ECR-Tonga Platform. The unstable nature of the southern Kermadec wedge under compression, together with a comparison of its taper characteristics with those of modern convergent margins, implies that the wedge deforms under a relatively high internal pore pressure but high effective basal friction regime. Strike-slip deformation in the wedge is attributable to a relatively strong interplate coupling related to the buoyancy and ruggedness of the Hikurangi Plateau.

1. Introduction

The subduction of thick buoyant oceanic plateaus or large aseismic ridges is likely to produce a major geologic impact on the overriding plate as it is generally inferred that the greater thickness of relatively light crust of the plateau will cause the plateau to resist subduction [*Vogt*, 1973; *Cloos*, 1993]. Large-scale geologic effects of the plateau subduction include the inhibition of backarc spreading, the formation of gaps or offsets in the volcanic line, the segmentation of the slab, and ultimately an orogenic collision and a reversal of subduction polarity when the subduction has been jammed by the collision [*Vogt et al.*, 1976; *Kelleher and McCann*, 1976; *McGeary et al.*, 1985; *Kroenke*, 1984]. A more localized consequence of the subduction of buoyant features is the isostatic uplift and deformation of the forearc region that occurs during the initial subduction of a thickened feature [*Cloos*, 1993] as illustrated by the deformation of the Panama-Costa Rica forearc landward of the subducting Cocos Ridge [*Corrigan et al.*, 1990; *Kolarski et al.*, 1995] and that of the New Hebrides forearc landward of the d'Entrecasteaux Zone [*Moretti and Ngokwey*, 1985]. Robust tectonic erosion of accretionary wedges and crystalline forearc regions also arises from the subduction of ridges [*McCann and Habermann*, 1989; *Von Huene and Lallemand*, 1990] and plays a significant role in the decrease of island arc and continental crustal mass [*Von Huene and Scholl*, 1991; *Lallemand*, 1995]. Detailed multibeam bathymetric and seismic reflection investigations [*Fisher et al.*, 1991b; *Pelletier and Dupont*, 1990a; *Von Huene and Culotta*, 1989; *Cadet et al.*, 1987] together with physical and experimental modeling [*Lallemand and Le Pichon*, 1987; *Geist et al.*, 1993; *Lallemand et al.*, 1994] have shown that ridge subduction produces substantial shortening of the inner trench wall followed by subsidence and collapse of the inner trench wall and a landward retreat of the trench. Folding, thrusting and subsequent collapse are enhanced when the subducting ridge creeps along an arc, parallel to the trench, as shown at the Louisville Ridge/Tonga arc collision zone [*Ballance et al.*, 1989; *Pelletier and Dupont*, 1990a; *McLeod*, 1994] and the d'Entrecasteaux Zone/ New Hebrides Arc [*Collot and Fisher*, 1991; *Fisher et al.*, 1991a]. However, the tectonic processes that control the structural development of a forearc in response to the subduction of a large oceanic plateau have been poorly documented. In this study, we use swath bathymetry, side-scan sonar imagery, and seismic reflection data to investigate the structures and to interpret the tectonic variations of the inner wall of the South Kermadec Trench as a

Paper number 97JB02474.
0148-0227/98/97JB-02474$09.00

consequence of the oblique subduction of the oceanic Hikurangi Plateau (Figure 1).

The Kermadec subduction zone (Figure. 1) is part of the convergent Pacific-Australian (PAC-AUS) plate boundary that extends for more than 2500 km along the Tonga-Kermadec Trench to the Hikurangi Trough in New Zealand. The associated convergence becomes progressively more oblique to the south, and near 37-38° S, the plate boundary undergoes a transition from intraoceanic subduction in the north to ocean-continental subduction in the south. The Hikurangi Plateau,

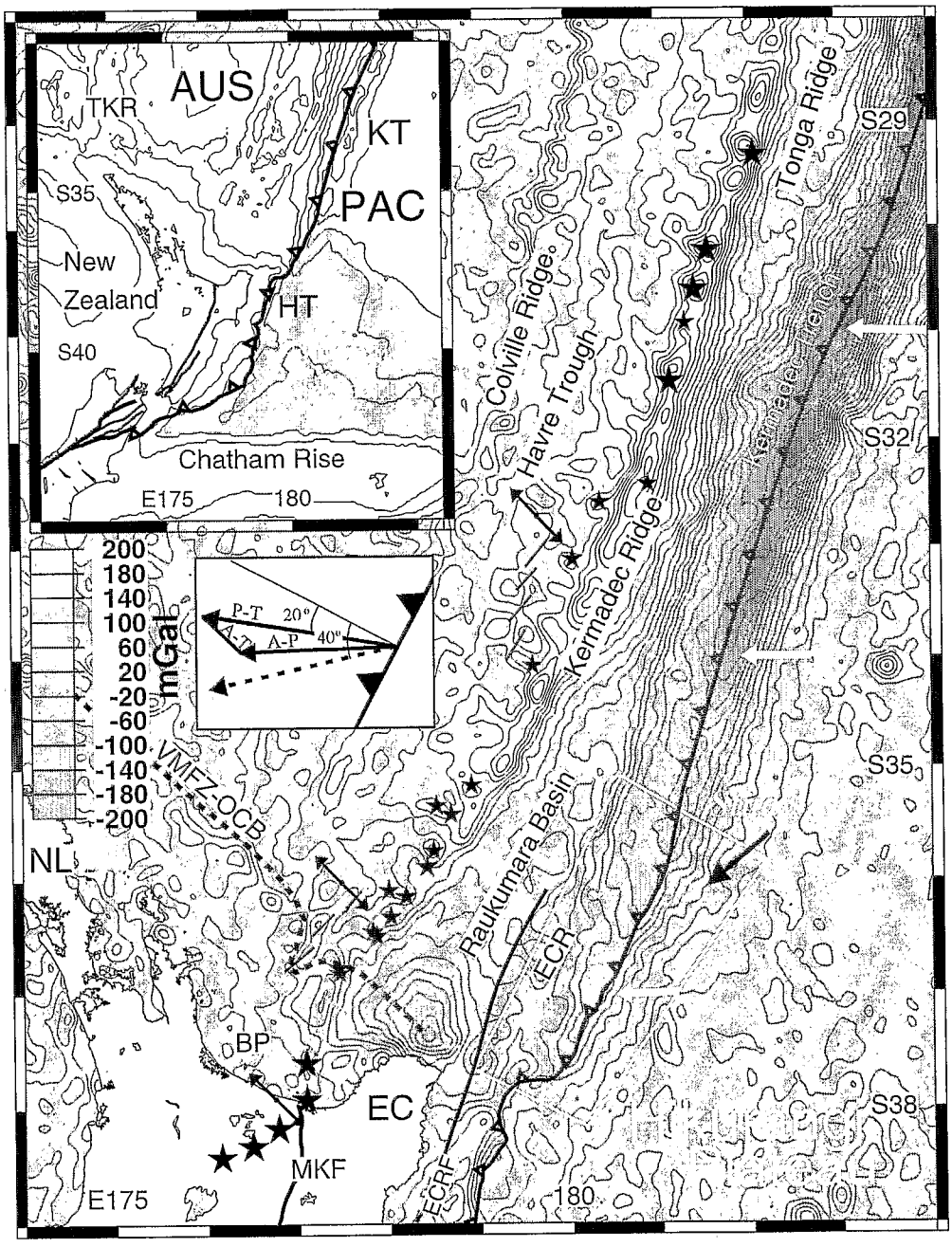

Figure 1. Satellite-derived marine gravity anomaly along the Kermadec Trench (*Sandwell and Smith* [1994]; contours every 20 mGal) and location of the study area. EC, East Cape; NL, Northland; VMFZ-OCB, Vening Meinesz Fracture Zone-Ocean / Continent Boundary; BP, Bay of Plenty; MKF, Mohaka Fault; ECRF, East Cape Ridge Fault [*Davey et al.*, 1997]; aerial volcanos of the Kermadec island arc are shown by the large stars; small stars are submarine volcanos. Note the westward offset of the volcanic line south of 32° 25'S. En echelon line segments in the Havre Trough are interpreted axial rift segments [*Wright*, 1993], and opposite arrows are direction of extension from focal mechanisms [*Pelletier and Louat*, 1989; *Anderson et al.*, 1995]. Open arrows are Pacific-Australia plate convergence direction from *de Mets et al.* [1990]. The large inset is a simplified bathymetric map that shows the extent of the Hikurangi Plateau; the line with teeth along the Kermadec Trench (KT) is the deformation front at which the Pacific (PAC) and Australia (AUS) plates meet. HT: Hikurangi Trough; TKR: Three Kings Ridge. The small inset shows the plate motion vector summations for the Pacific-Tonga/Kermadec (P-T), Australia-Tonga/Kermadec (A-T), and Australia-Pacific (A-P) plates at 37° S. The direction of the estimated A-P vector at 5 Ma prior to Havre Trough opening is indicated by the dashed vector.

which underthrusts both the southern Kermadec forearc and the Hikurangi margin, is a 1000-km-wide, triangular high-relief (1-3 km) oceanic plateau that has its northern apex located in the Kermadec trench near 36° S (Figure 1) [*Davy*, 1992]. The oblique subduction of the plateau [*Katz*, 1982; *Lewis and Pettinga*, 1993] requires the accommodation of a margin-parallel component of relative plate motion, which is expected to have produced either oblique structures or strike-slip faults in the forearc, depending on the degree of strain partitioning [*Fitch*, 1972; *McCaffrey*, 1992; *Teyssier et al.*, 1995; *Ryan and Coleman*, 1992].

2. Geological Setting of the Hikurangi Plateau

The Hikurangi Plateau is a 12-15-km thick volcanic plateau [*Davy*, 1992] that is separated from normal, 8-km-thick Pacific oceanic crust [*Houtz et al.*, 1967] along its northeastern boundary by the 1-km-high Rapuhia Scarp. Geosat gravity anomalies [*Sandwell and Smith*, 1994] (Figure 1) and gravity modeling by *Davy* [1992] and *Davy and Wood* [1994] indicate that the plateau is isostatically compensated and bounded along the Rapuhia Scarp by an abrupt crustal fault. Buoyancy calculations by *Cloos* [1993] indicate that basaltic oceanic plateaus thicker than 17 km should resist subduction. Although the Hikurangi Plateau is subducting, its 15-km-thick crust may, depending upon its bulk density (basalt versus amphibolite), be close to the boundary where the role of the buoyancy reverses from driving to resisting subduction.

Much of the plateau apparently formed in the Mesozoic [*Strong*, 1994] with volcanic peaks of Cretaceous or older ages [*Wood and Davy*, 1994]. Some intrusives, however, may have been emplaced in late Miocene to Recent times [*Lewis and Bennett*, 1985]. Dredging from the basement of the plateau at the Rapuhia Scarp sampled normal to enriched mid-oceanic ridge basalt (N- to EMORB) with geochemical characteristics similar to those reported from early Cretaceous oceanic plateaus in the western Pacific [*Mortimer and Parkinson*, 1996]. *Wood and Davy* [1994] divide the plateau into several regions on the basis of basement structure and sedimentary cover. The northern volcanic region that is presently underthrusting the southern Kermadec margin shows widespread volcanic peaks and a shallow volcanic basement overlain by a thin (<1 s) sedimentary cover. This cover is interpreted as a condensed sequence of Late Cretaceous and Paleogene age. On the basis of seismicity and gravity modeling, the plateau is being subducted at a 5-7° dip for 200 km west of the trench [*Reyners*, 1989; *Davy*, 1992].

Bathymetric data in the study area reveal some characteristics of the Hikurangi Plateau that have implications on the structural development of the inner trench wall. The seafloor of the plateau that is adjacent to the South Kermadec Trench dips regionally northeastward from 3.7 km in the south to 5.5 km in the north. This change in elevation combined with a 20° obliquity of the convergence suggests that an area of the inner trench wall that is initially uplifted by the underthrusting of the highest region of the plateau will subside when this region withdraws southwestward. Other characteristics of the plateau in the survey area include three small ridges that trend at high angle to the plate boundary, as well as bending-induced normal fault scarps, which reach 400-500 m in height and are better developed in the northern part of the survey area than in the south [*Collot et al.*, 1996]. The dominant fault trend is N-S to N20° E and oblique to the trench. A secondary N45°-60°E trend is marked by scarps and slopes. A feature of the South Kermadec Trench that is critical for the evolution of the inner trench wall is the lack of trench fill sediment which is in turn attributable to the transport of turbidites along the Hikurangi Trough being diverted eastward before they reach the trench [*Lewis*, 1994].

3. Geodynamic and Kinematic Setting of the Kermadec Subduction Zone

The subduction of the PAC plate beneath the AUS plate has been active along the Kermadec Trench for more than 40 Myr forming successively the Three King Ridge, the Colville Ridge, and the Kermadec Ridge [*Walcott*, 1987]. The Colville and Kermadec Ridges are interpreted to have been a single volcanic arc prior to initial rifting of the Havre Trough, 4-5 Myr ago [*Karig*, 1970; *Wright*, 1993].

The obliquity of the convergence along the Kermadec Trench reaches 30° at 37°S and the convergence rate between the PAC and AUS plates decreases from 6.3 cm/yr near 30°S to 4.9 cm/yr at 37°S [*de Mets et al.*, 1990]. The forearc tectonics are, however, more directly determined by the convergence vector between the PAC plate and the Tonga-Kermadec (TK) microplate. This vector is the sum of the PAC-AUS plate vector and the AUS-TK divergent vector [*Pelletier and Louat*, 1988] associated with Havre Trough rifting. The resulting PAC-TK vector is 20° oblique to the plate boundary and reaches 6.0 cm/yr at 37°S (Figure 1). This vector provides a good estimate of the regional convergence over the last 4-5 Myr, i.e., since the initiation of the Havre Trough extension. Before 5 Ma, the convergence vector was more oblique (40°) to the plate boundary (Figure 1) because the 5-10 Ma PAC-AUS stage pole of rotation was located north of its present location [*Sutherland*, 1995].

The Kermadec Ridge is highly magnetic [*Kibblewhite and Denham* 1967] and consists of a thick (> 4 km) pile of volcanoclastic sediment [*Dupont*, 1982] with a basaltic-andesitic rock core [*Cole*, 1986]. The active volcanic arc forms a series of emergent, basaltic to low-K basaltic-andesitic volcanoes [*Cole*, 1986] that cap the Kermadec Ridge. South of 32°S, island arc volcanoes become submarine and shift 15-25 km westward with respect to the ridge axis into the backarc domain [*Wright*, 1994] (Figure 1).

In spite of its early recognition as part of a major convergent plate boundary [*Karig*, 1970], the structure of the Kermadec forearc has remained poorly constrained because of a lack of modern geophysical data. Using seismic reflection reconnaissance profiles, *Pelletier and Dupont* [1990b] show a drastic change in morphology and structure of the steeply dipping forearc slope at 32°S. North of 32°S, they interpret tectonic erosion along the inner wall of the trench related to a high degree of roughness on the downgoing plate, whereas south of 32°S, they recognized localized tectonic accretion associated with a smooth adjacent outer trench wall.

From 34°S southward, the forearc classically comprises [*Karig and Sharman*, 1975] a forearc basin (the Raukumara basin), an outer arc structural high (the East Cape Ridge), and an inner trench wall that appears to lack an actively growing accretionary wedge. The forearc basin lies under 2400 m of water and contains 4-6.5 km of Cenozoic and Quaternary

sediment [*Katz*, 1974; *Gillies and Davey*, 1986]. These sediments are distributed over a basement that forms part of the East Cape Ridge and may include oceanic crust [*Gillies and Davey*, 1986]. The four sedimentary units recognized in the basin indicate several episodes of filling of the basin and uplift of the East Cape Ridge associated with a transverse migration of the depocenter [*Gillies and Davey*, 1986]. Examination on seismic reflection profiles from *Gillies and Davey* [1986] of the upthrust eastern part of the deepest unit, which is inferred to be at least 5 Ma old, shows evidence of deformation and erosional truncation of the unit strata over the East Cape Ridge, suggesting that the ridge has been tectonized and could have been emergent in the past.

The transition zone between the oceanic domain of Raukumara Basin- East Cape Ridge, and the North Island continental margin has had a complex geological history that has important implications for the present-day tectonics of the forearc region. At about 25 Ma the sedimented- passive margin of North Island, which extended from Northland to East Cape (Figure 1) became the locus of oblique subduction [*Ballance*, 1976, 1993] that initiated with the obduction of Cretaceous and Paleogene oceanic crust and sediment onto East Cape and Northland [*Strong*, 1980; *Rait et al.*, 1991]. A northward dipping root of this Cretaceous ophiolite has been inferred to underlay the southern Raukumara Basin [*Davey et al.*, 1997]. *Mortimer and Parkinson* [1996] proposed that this ophiolite may have been derived from volcanics of similar chemistry on the Hikurangi Plateau which were obducted following collision of the plateau in the early Miocene. By early to mid-Miocene the Vening Meinesz Fracture Zone (VMFZ) (a dextral continent-ocean transform fault zone, trending northwest) became active along the eastern margin of Northland [*Herzer and Mascle*, 1996] suggesting that, at this time, the paleo-Kermadec trench was located farther west relative to North Island [*Davey et al.*, 1997]. During the mid-Miocene a northeast trending, oblique convergent plate boundary developed along the North Island eastern margin [*Walcott*, 1987; *Herzer*, 1995]. The southeasternmost extremity of the VMFZ may have reached and faulted transversally the present-day forearc region, immediately northeast of East Cape. In addition to transverse faulting, the South Kermadec forearc region likely experienced the brunt of longitudinal transcurrent-faulting that developed during the Miocene along the eastern margin of North Island in association with oblique convergence [*Delteil et al.*, 1996]. Strike-slip faulting continued during the Neogene along the Mohaka Fault (Figure 1) [*Cutten*, 1994]. The East Cape Ridge Fault imaged offshore East Cape from seismic reflection data has been interpreted as a major northeast trending, dextral transcurrent fault [*Davey et al.*, 1997]. Oblique subduction during the Miocene also produced up to 30° of clockwise rotation of crustal blocks along segments of the continental plate boundary [*Lamb*, 1988; *Walcott*, 1989].

The inner trench wall shows large-scale changes in tectonic style along the Kermadec and Hikurangi margins. From a preliminary interpretation of multibeam bathymetric data, *Collot et al.* [1996] show that the South Kermadec Trench and its inner wall extend from the Rapuhia Scarp in the north to the Ruatoria Scarp in the south at 37°45'S (Figure 2). The trench segments located immediately north and south of the South Kermadec Trench are laterally offset westward by 15-25 km and contain turbidites, whereas the South Kermadec Trench lacks turbidite fill. Work in progress by the authors suggests that the northern trench offset results from the collapse of the toe of the margin in the wake of the Rapuhia Scarp subduction. The southern trench offset is inferred to be the result of collapse due to the repeated impact of large seamounts on the Hikurangi Plateau with the Hikurangi margin [*Lewis and Pettinga*, 1993; *Collot et al.*, 1996]. Between these two areas of collapse, the South Kermadec inner trench wall is split along-strike by a major fault, that we name the Awanui Fault (Figure 3). This highly tectonized margin recorded the geologic events associated with the oblique subduction of the Hikurangi Plateau and will be described in section 5.

4. Geophysical Data

SIMRAD EM12D multibeam bathymetric and side-scan sonar data, as well as six-channel seismic reflection profiles and geopotential data, were collected over the inner wall of the South Kermadec Trench and adjacent sector of the Hikurangi Plateau (Figure 2) during the GEODYNZ-SUD cruise of the R/V *L'Atalante* in November 1993. The EM12D multibeam bathymetric data have been reprocessed to a 100-m grid, which, when contoured at a 20-m interval, shows enhanced morphologic details of the large-scale features described in the initial report [*Collot et al.*, 1996] and also reveals new features. These features are interpreted using the above seismic reflection and side-scan sonar data (Figure 2). EM12D data were complemented by a few MR1 side-scan sonar and bathymetry swath lines acquired in September 1994 by the National Institute of Water and Atmospheric Research and Seabed Mapping New Zealand Ltd. along the upper trench slope. MR1 bathymetric data contain an artefact that follows the medium line of the swath and which could not be totally removed. The 20-m-contoured EM12D bathymetric maps also displayed some local artefacts that are transverse to the ship tracks. To remove these artefacts, EM12D data were regridded at 175 m and filtered numerically. These data were then merged with filtered MR1 bathymetry and contoured at 25-m intervals to produce figures 3, 4, 5, and 6,

The survey was designed to optimize the multibeam data collection so the seismic reflection data were shot in a nonoptimum direction, parallel to the margin. These seismic reflection data, produced by two 75 cubic inch in GI air gun sound sources operating in harmonic mode, have been processed through threefold stack and migration with a basic constant velocity function below seafloor. The resulting profiles have been used to correlate structures along the margin. Other seismic data used in this study (Figure 2) include multichannel and single-channel profiles obtained by Mobil and Gulf in 1972, single-channel profiles acquired on the R/V *Tangaroa* in late 1980 [*Gillies and Davey*, 1986], and a 160-channel seismic reflection line obtained by the R/V *Explora* in December 1990 [*Davey et al.*, 1997]. Part of the *Explora* line was reprocessed through to migration using a similar velocity function to that employed on the *L'Atalante* data. This reprocessed section shows internal structures of the inner trench wall (Figure 7). From these data, we focus on the detailed morphostructure of the South Kermadec inner trench wall (Figure 8) and investigate the tectonic mechanisms of disruption of the margin. We then derive evidence for variations in the tectonic regime and large-scale tectonic erosion processes that are produced by the oblique subduction of the Hikurangi Plateau.

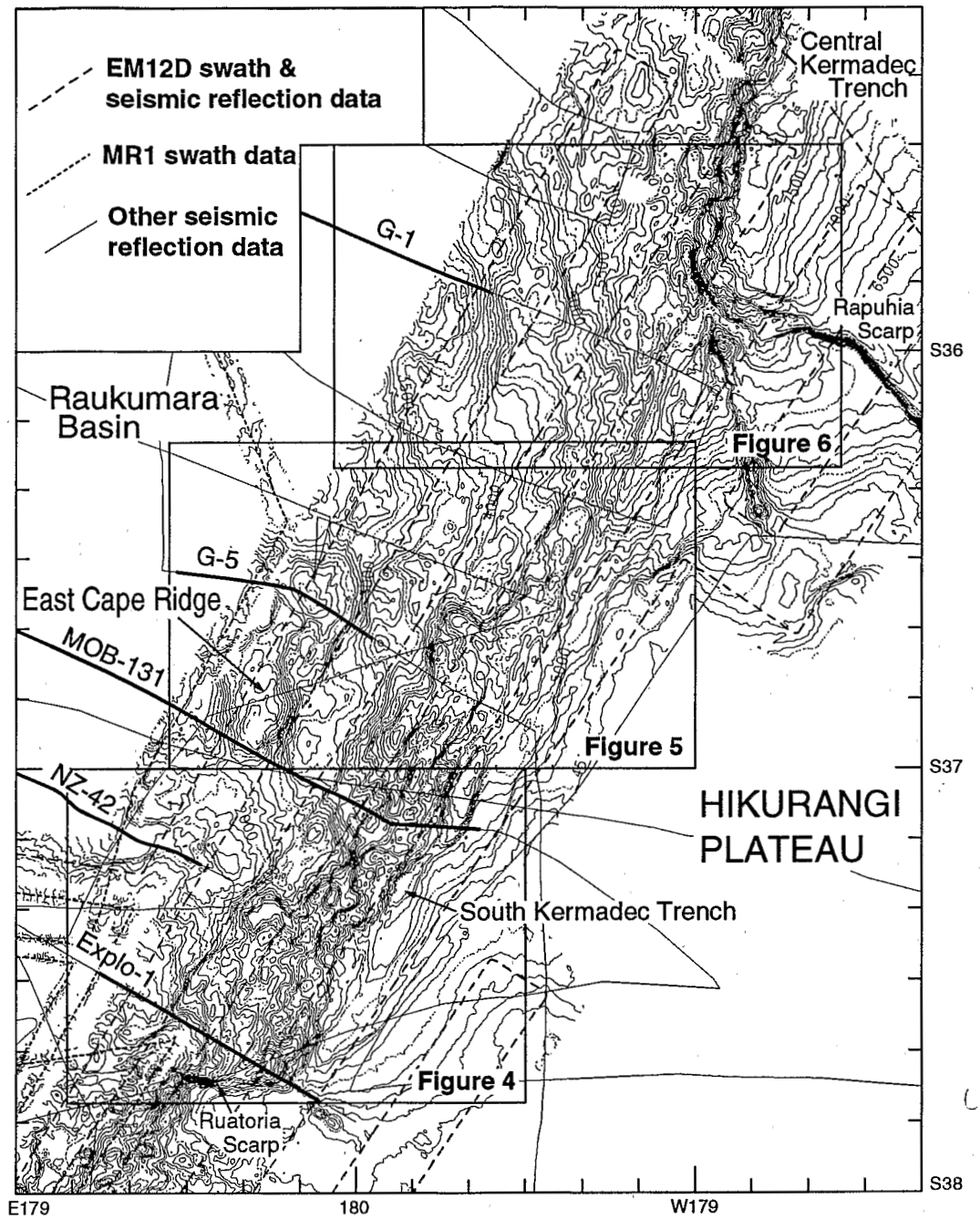

Figure 2. Swath bathymetric map compiled from available EM12D and MR1 data showing seismic reflection profiles used in this study. Bathymetry contours are every 100 m.

5. Structure of the Southern Kermadec Inner Trench Wall

The seafloor morphology reflects the major structural elements of the inner wall of the South Kermadec Trench as indicated by seismic reflection profiles described below. On the basis of multibeam bathymetry and seismic data we divided the inner trench wall into structurally distinct upper, middle, and lower parts that trend roughly parallel to the trench (Figure 8). From west to east, the morphostructure of these three parts can be described as follows:

5.1. Upper Part of the Margin

The upper part of the margin comprises the northeastern corner of the North Island continental margin south of 37°10'S, and the East Cape Ridge that projects northeastward from this latitude (Figures 2 and 8). On the basis of regional bathymetric, magnetic and petrological data, *Wright* [1993] has identified a NW trending continent-oceanic boundary within the Bay of Plenty to the west of the Raukumara Basin (Figure 1). This boundary is associated with the VMFZ and coincides with the 2200-m isobath at the toe of the continental slope. In the study area, the northern boundary of

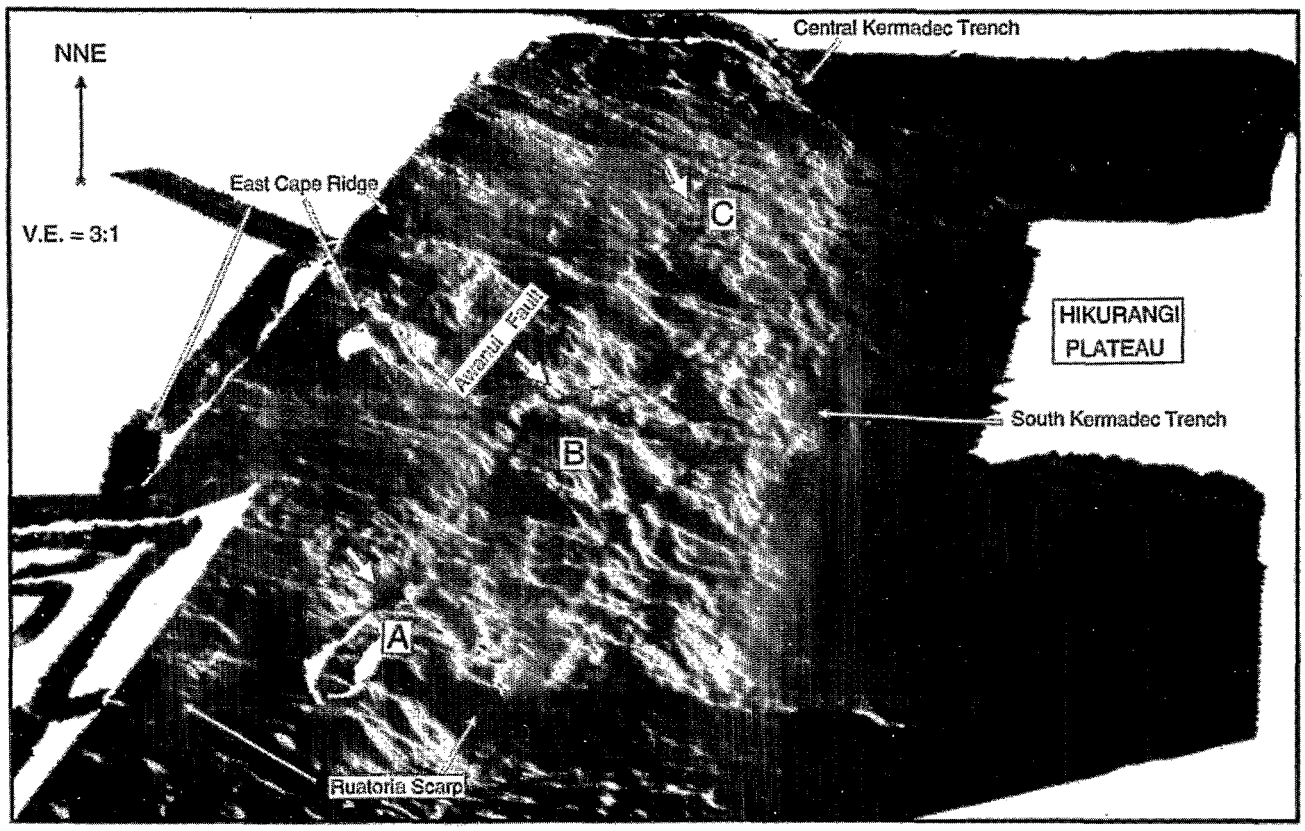

Figure 3. Shaded perspective-bathymetric diagram of the South Kermadec Trench looking north-northeast; illumination is from the east; vertical exaggeration is 3:1; A, B, and C are structural blocks described in text.

East Cape crust shows two prominent scarps, whose location and trend coincide with the southeastward projection of the VMFZ. The shallowest one, at a depth of 1500 m, is 300-m high and trends WNW (S1 in Figures 4 and 8). The deepest one (S2) is a 400-m-high, E-W trending scarp that marks the base of the northern slope near 2100 m, a depth that is similar to that of the continent-ocean boundary in the Bay of Plenty. This E-W trending scarp may mark the toe of the continental margin.

The eastern side of the continental corner bounded to the north by scarp S2 is outlined by a N30°E trending fault scarp as far south as 37°20'S, south of which both the upper and middle parts of the margin merge. The fault scarp may indicate an apparent right-lateral offset of the E-W trending side of the continental corner. The multichannel seismic reflection line Explo-1 [*Davey et al.*, 1997] that cuts across the margin (Figure 7) shows that the upper and middle parts of the margin consist of a deformed acoustic basement overlain by a layer of acoustically transparent sediment and a stratified sequence. This sequence shows numerous channels filled with sediment but no evidence for recent tectonic deformation that could correlate with the strike-slip fault hypothesized farther north. However, *Davey et al.* [1997] interpret the East Cape Ridge (ECR) Fault, immediately west of the study area, as a major recently active, dextral transcurrent fault (Figure 8).

The ECR consists of several rounded or flat-topped highs, which deepen northeastward from 1500 m in the south to 3800 m in the northern part of the survey area. The ridge is shallower than the adjacent Raukumara forearc basin between latitude 37°05'S and 36°20'S. Farther north, the ridge is deeper than the adjacent forearc basin. Multibeam bathymetry and seismic reflection data described below indicate that the deformation of the East Cape Ridge and its western flank varies from transpressive south of 36°40'S to extensional north of this latitude (Figure 8). Near 37°10'S, and immediately north of S1, the boundary between the ECR and the North Island continental slope is marked by an E-W elongated, 10-km-wide trough (Figures 4 and 8), which runs into the Raukumara Basin. Bathymetric and MR1 imagery data (Figure 9) show NE trending lineaments that cut at a high angle to the continental margin in the south and extend discontinuously across this trough and northward along the ECR. In the trough the lineaments are arcuate and en echelon. Seismic reflection line NZ-42 (Figure 10) and other seismic data across the upper part of the margin (Figure 2) indicate that the sediments in the E-W trending trough are deformed by folds and steep reverse faults that verge both east and west and can be interpreted as a flower structure. These features deform the seafloor and correlate with the discontinuous, sinuous lineaments mentioned above (Figure 9). Farther north, seismic reflection line MOB-131 (Figure 11) shows that forearc basin sediments along the ECR western flank are faulted and folded to form a positive flower structure. The seismic line also shows that the ridge crest is dissected by steeply dipping faults. Both seismic lines MOB-131 and NZ-42 show a similar steep fault zone, located 10-20 km west of the ECR in the fore-arc basin sediment, with vertical offset of the seafloor upthrown on the west side, which may be the northward continuation of the dextral, transcurrent, East Cape Ridge Fault of *Davey et al.* [1997].

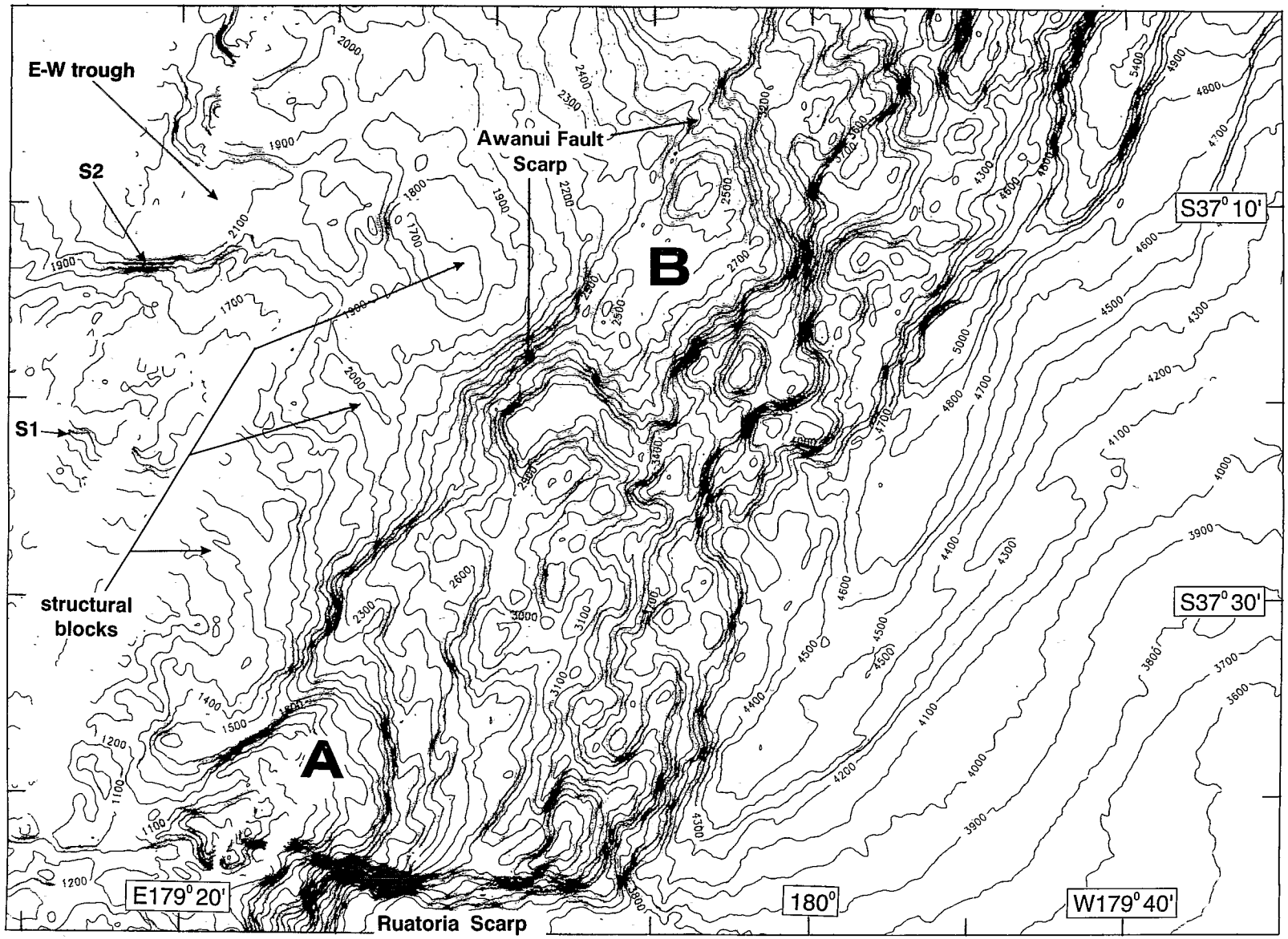

Figure 4. Multibeam bathymetric map of the southern part of the South Kermadec Trench; contours are 25 m. S1 and S2 are fault scarps, and A and B are structural blocks described in text. Location as shown in Figure 2.

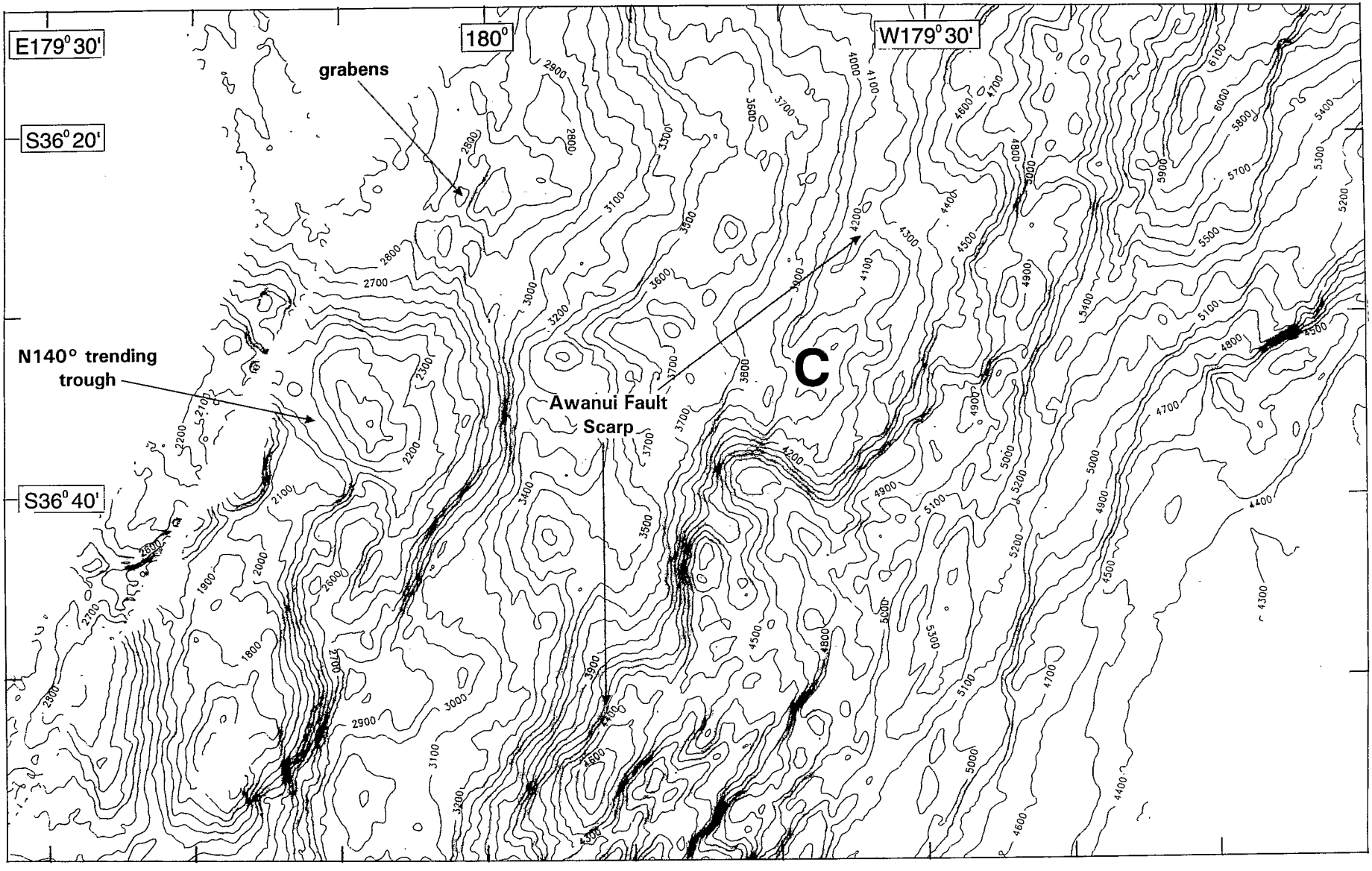

Figure 5. Multibeam bathymetric map of the central part of the South Kermadec Trench; contours are 25 m. Location as shown in Figure 2. C is structural block described in text.

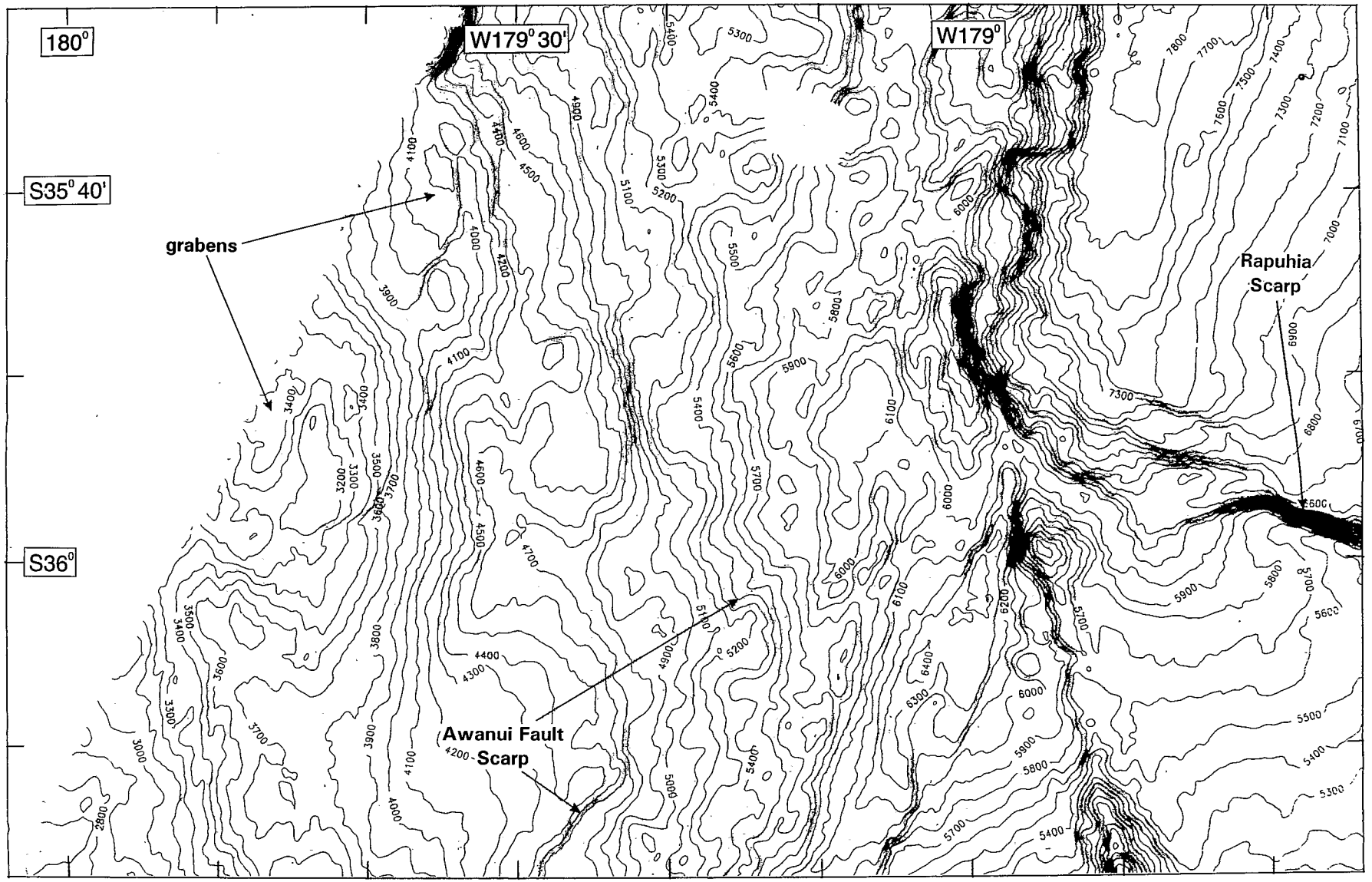

Figure 6. Multibeam bathymetric map of the northern part of the South Kermadec Trench; contours are 25 m. Location as shown in Figure 2.

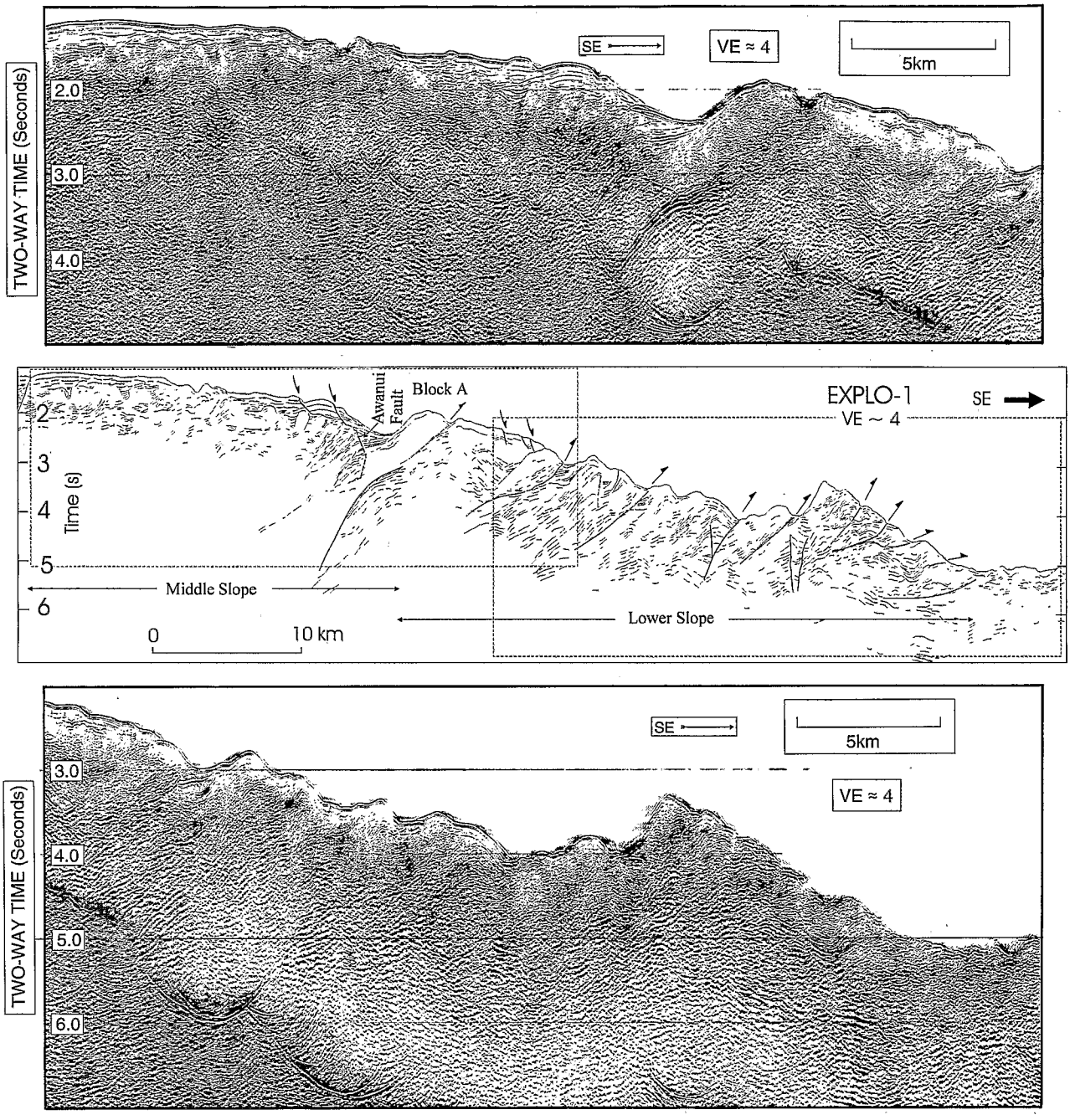

Figure 7. Seismic reflection line Explo-1 with line drawing; location is shown in Figure 2. The overmigrated water bottom multiple is obvious on both seismic sections.

The western flank of the ECR bulges westward at 36°40'S and consists of deformed stratified sediments of the forearc basin, which terminate eastward against a major fault zone (line G-5, Figure 12). These sediments are deformed by a network of subvertical or slightly reverse faults, with small, west facing throws that are convex westward in plan view (Figure 13) and truncate southward against a major NE trending fault. Therefore, although the quality of the seismic line makes clarification of the nature of the faults difficult, the map view geometric relationships of the faults show that the faults are steeply dipping reverse faults and part of a flower structure that developed in a compressional environment. The overall combination of morphology, imagery, and seismic reflection data along the segment of the ECR south of 36°40'S indicates active transpressive deformation.

Near 36°40'S the ECR is cut transversally by a N140°E elongated trough (Figure 5), north of which the ridge is cut along strike by an interpreted trenchward facing fault scarp that splays north-northeastward into a network of sinuous fault scarps incising the ridge summit (Figure 14). These latter scarps delineate and bound a series of shallow structural troughs trending subparallel to the ECR. We interpret this morphology as indicative of a summital zone of grabens. North of 36°S seismic reflection line G1 [*Gillies and Davey*, 1986] (Figure 15) and bathymetric data indicate a 10-20-km-wide graben that is deeper than the forearc basin, from which

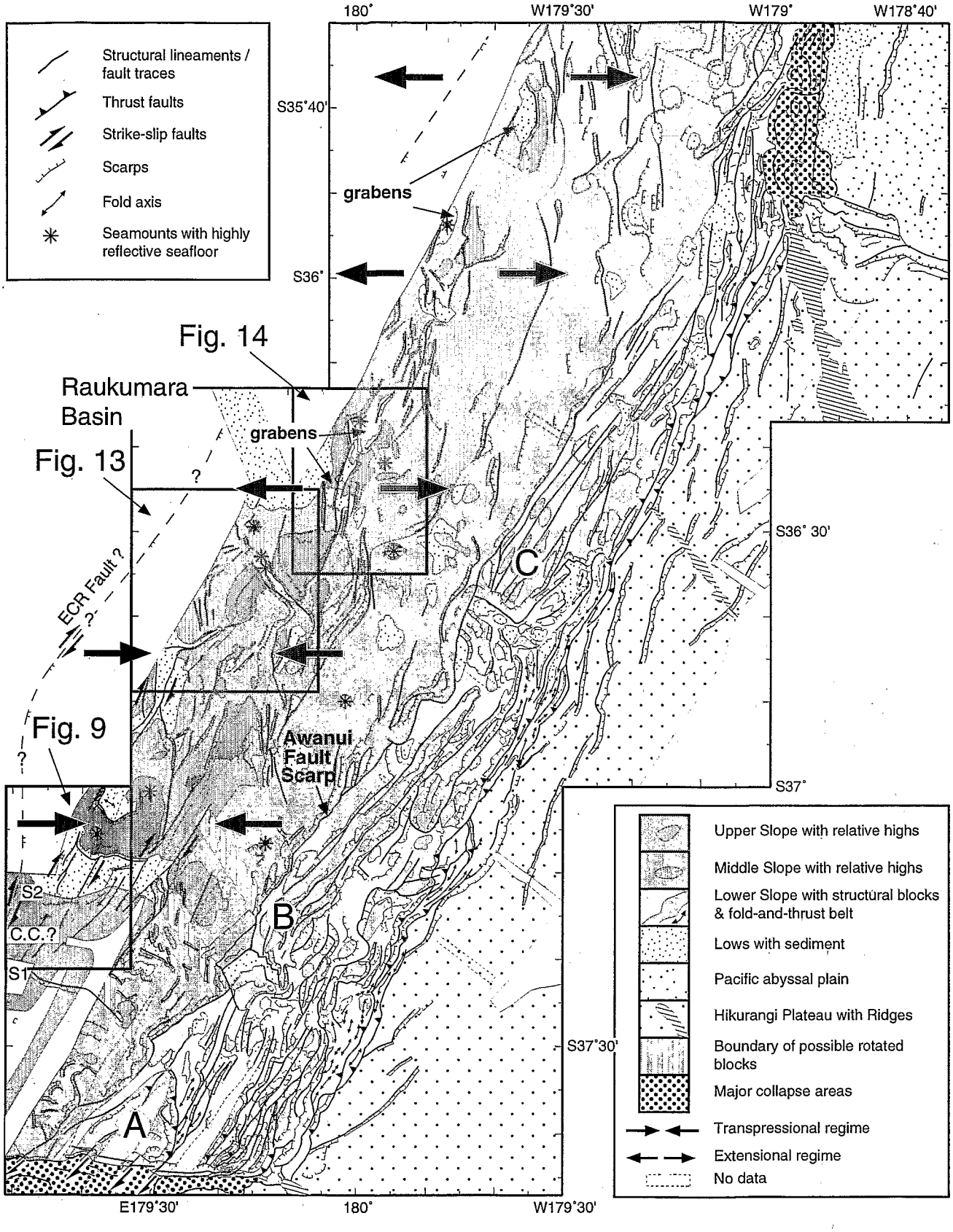

Figure 8. Structural map of the South Kermadec Trench interpreted from multibeam bathymetry, side-scan sonar imagery, and seismic reflection data; S1 and S2 are scarps discussed in text; C.C. is continental corner; A, B, and C are structural blocks described in text.

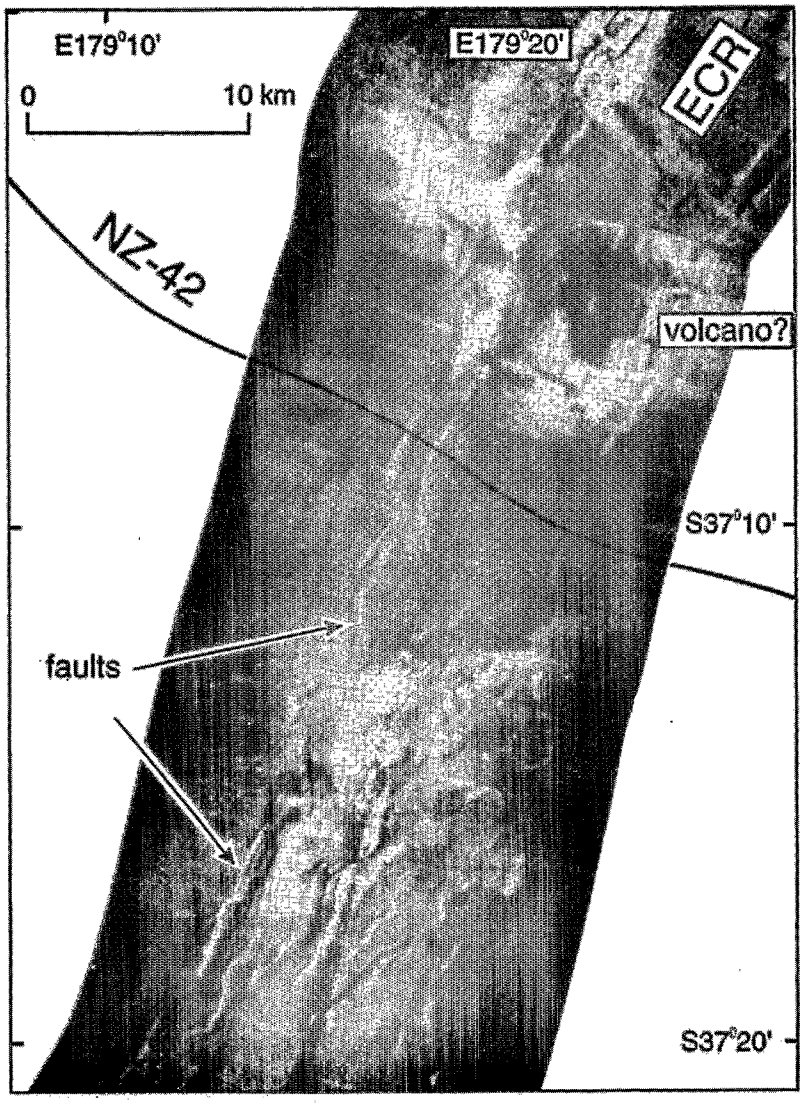

Figure 9. MR1 side-scan sonar imagery of the junction between the continental New Zealand margin and the East Cape Ridge. Location and interpretation are in Figure 8.

the graben is separated by a 0.7-1 km normal fault scarp. The detailed bathymetric data reveal at least two other small grabens which lie on the inner trench slope north of 36°S (Figures 6 and 8). They are bounded trenchward by elongated highs that have an arcuate, concave upslope shape, suggesting that these graben were tilted trenchward as the slope subsided.

Several enigmatic, small-sized (50-300 m in height, 2.5-3.5 km in diameter) seamounts were mapped along the ECR. These seamounts, marked by stars in Figure 8 and open triangles in Figure 16, have strongly reflective seafloor. The largest one resembles a volcano surrounded by lava flows (Figure 9). It lies in the transpressive fault zone of the ECR and is associated with a regional magnetic anomaly (Figure 16). Three others are small mounds that line up along the axis of the transverse graben (Figures 5 and 13) and two others lie in the grabens north of 36°40'S and are therefore associated with extension. In absence of other data, these seamounts, which are located only 65 km west of the trench, can be interpreted either as volcanic intrusions [*Taylor*, 1992; *Bloomer et al.*, 1994], mélange diapirs [*Orange and Underwood*, 1995] or serpentinite bodies [*Fryer et al.*, 1985].

5.2. Middle Part of the Margin

The middle part of the margin forms an elongate, 15-20-km-wide terrace that deepens irregularly northeastward (Figures 17, 18 and 19). This part is separated from the upper part by steep scarps and slopes of the ECR eastern flank and from the lower part by the Awanui Fault scarp and lineament. The terrace shows few structures in comparison with the upper and lower parts. It is transversally flat with slope angles between 0° and 1.5° (Figure 18) and is locally pierced by small reflective seamounts similar to those discovered on the upper part of the margin. South of 37°10'S three structural blocks about 20 km wide can be interpreted from the morphologic data (Figures 4 and 8). These blocks are located between the Awanui scarp and the transpressive fault zone of the ECR. They are bounded on their northeast and southwest sides by a N150°E structural grain that matches with left-stepping

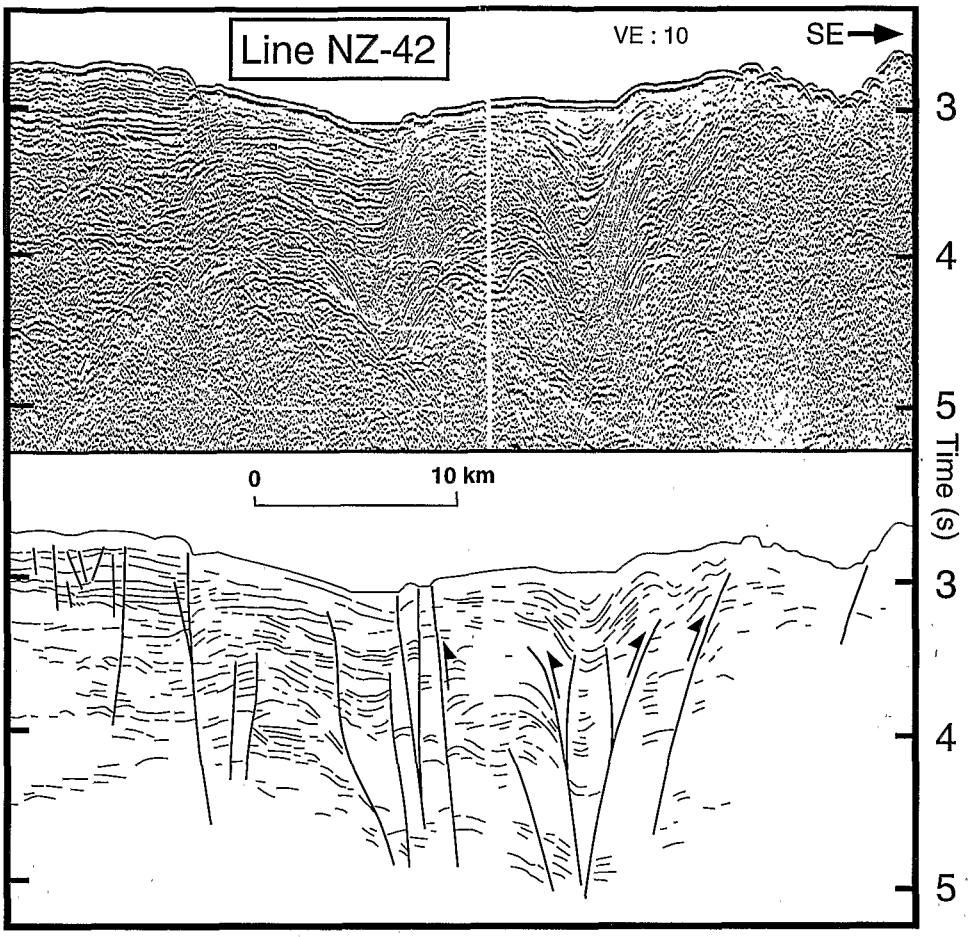

Figure 10. Seismic reflection line NZ-42 with line drawing; location is shown in Figures 2 and 9.

segments of the Awanui Fault. The central block appears to be depressed relative to the northern and southern ones.

5.3. Lower Part of the Margin

The lower part of the margin between the Awanui Fault scarp and the tectonic front narrows northward from ~40 km wide near the Ruatoria Scarp to ~20 km in the north (36°10'S) (Figures 3 and 8). The highest part of the Awanui Fault scarp, which south of 37°S shows several left-stepping offsets, can be traced for 150 km from 37°40'S to 36°40'S. Multibeam bathymetric data (Figures 5 and 6) indicate that the Awanui Fault extends farther north to 36°S along a 150-m-deep valley that is aligned with a series of SE facing scarps. The fault trace reaches a total length of nearly 220 km.

The lower part of the margin contrasts strongly with the two other parts. It divides along- strike into three elongated, NE dipping, highly deformed, slope segments separated by prominent, rectangular, ~10 km wide, ~500 m deep, bathymetric lows (Figures 4, 5, and 19). The three slope segments comprise respectively structural blocks A, B, and C (Figures 3, 8 and 19). These blocks, defined by massive and rough morphologic highs fault-bounded to the west and south, have differing morphostructural characteristics.

Multichannel seismic reflection line Explo-1 across structural block A shows that the lower part of the margin is an actively deforming imbricated sedimentary wedge (Figure 7). The interplate décollement is not imaged as a strongly reflective seismic interface but is suggested to extend westward from the trench between 5 and 6 s two-way-time (TWT) along a chaotic zone of reflections. The wedge consists of multiple, seismically reflective thrust sheets that are complexly deformed by folds and steeply dipping faults and separated by east verging thrust faults. A well-imaged thrust fault outcrops at the seafloor (~3 s TWT) at the base of the trenchward flank of a 10-km-wide bulge at the crest of block A, indicating that the bulge is a compressional feature. In addition to compression, the morphologic data show that some of the reverse and thrust faults in the wedge have a trench-parallel, dextral, strike-slip component as indicated by small (1-2 km) lateral offsets across the Ruatoria Scarp immediately south of line Explo-1 (Figure 8).

A positive 150-nT magnetic anomaly (Figure 16) centered on the Ruatoria Scarp, ~15 km south-southeast of the above bulge may be attributable to the presence of a subducted seamount as indicated by magnetic modeling [*Davey et al.*, 1997]. The long-wavelength character of the seismic reflection record deeper than ~3.0 s TWT beneath the bulge on Figure 7 may reflect basement rocks of the buried seamount rather than sedimentary layers. A set of strong and steeply landward dipping reflections underlie the western flank of the bulge and may mark the leading flank of the postulated subducting seamount. Such a seamount could account for much of the uplift of the bulge by compressing sedimentary layers

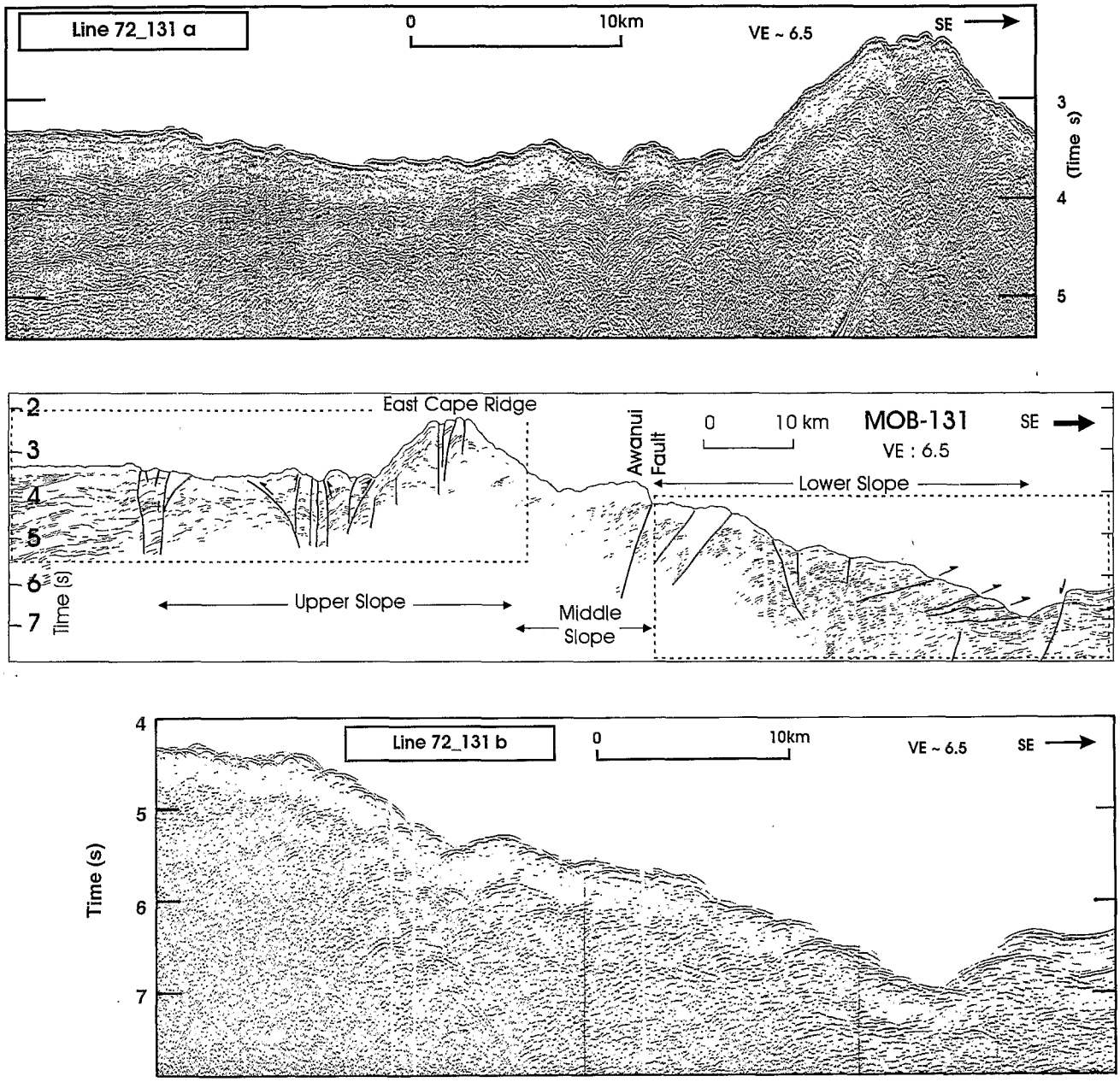

Figure 11. Seismic reflection line MOB-131 with line drawing; location is shown in Figure 2.

against the Awanui Fault which appears to be steeply west dipping at depth (Figure 7). Alternatively these reflections may mark a steeply west dipping reverse-fault associated with the Awanui Fault.

The two northern slope segments, which form structural blocks B and C are dominated by a strong NNE oriented structural grain. They consist of 5-10 km wide, 50-200 m amplitude ridges separated by linear valleys, SE facing scarps and morphologic lineaments. We interpret blocks B and C to be composed of rock slivers bounded by linear faults. On average, the slivers trend slightly oblique (5-10°) to both the Awanui Fault scarp and the deformation front suggesting that the slivers formed in a dextral-transpressive tectonic regime associated with oblique convergence. The summit of block B, located between 37°10' and 37°20'E, is shallower than the adjacent middle part of the margin (e.g. in profile 5, Figure 18) suggesting that because the Awanui Fault steps to the left near 37°16'E, the transpressive rock slivers are compressively uplifted against the Awanui Fault (Figure 20) due to a combination of "jammed" strike-slip motion along the Awanui Fault and the steep dip of this fault. The seaward flanks of blocks B and C are steep (12-20°) and show evidence for collapse along trenchward dipping normal faults. For example, near 37°18'S on the trenchward flank of block B, two fault traces, arcuate in map view, can be interpreted from slope breaks (Figures 4 and 8). The fault traces are concave upslope, suggesting that the faults are normal. Normal faulting, the subsequent subsidence of microblocks, and collapse are all associated with an oversteepened outer flank of the blocks, which in turn result from oblique thrusting against the Awanui

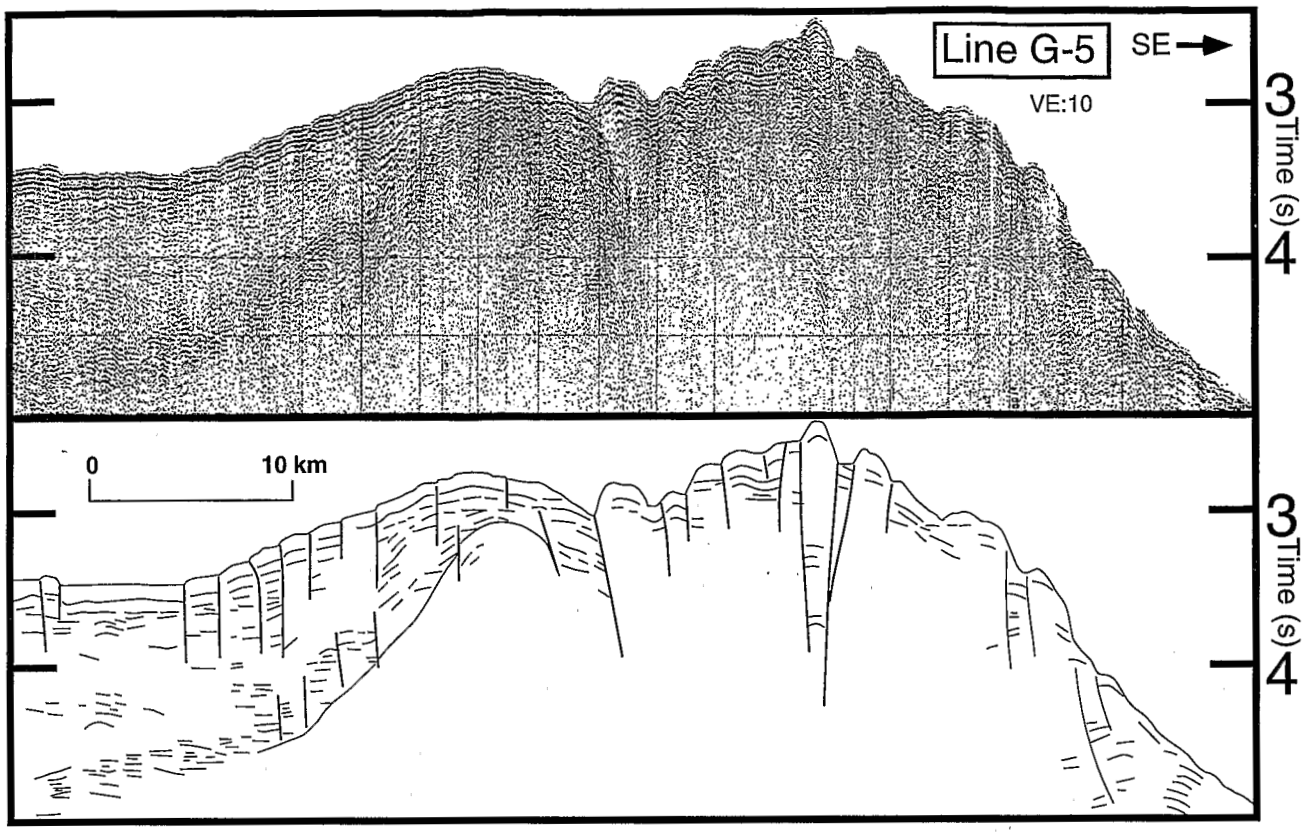

Figure 12. Seismic reflection line G-5 with line drawing; location is shown in Figures 2 and 13.

Fault. The southern part of Figure 20 illustrates our model of this process. The products of mass wasting largely accumulate at the toe of block B, as indicated by numerous, randomly spread, closed topographic highs and lows.

A narrow (1-10 km), small-amplitude fold-and-thrust belt (accretionary wedge), trending N28°E has developed discontinuously at the toe of the forearc slope. This belt, which is imaged on seismic reflection line MOB 131 (Figure 11), consists of small and thin thrust sheets. Near 36°S the structural direction of the fold-and-thrust belt sharply changes to N10° E thus truncating the rock slivers of structural block C. This change is related to the subduction of a ridge and normal faults of the Hikurangi Plateau (Figure 8).

The two deep bathymetric lows located, southwest of blocks B and C respectively (Figure 3), have different morphostructures, but both were produced by strike-slip tectonics: the southern low by rotation and the northern low by translation, as discussed below. The northern low at 36°40'S (Figure 5) forms a 4700-m-deep morphologic reentrant, which truncates and therefore postdates the formation of the NE trending slivers of block C. The truncation occurred along a SW facing, 500-m-high, N127°E trending wall. The reentrant is bounded westward by the 1000 m-high Awanui Fault scarp and has a 400-800-m-high N-S trending scarp at the southern border. East of this southern border, the northern extremities of rock slivers of structural block B are truncated and deflected toward the reentrant. Rock slivers on the opposing southern limit of block C show no corresponding westward deflection. The seafloor of the reentrant comprises closed lows and highs, and a N125°E, 500m-high ridge that connects at a right angle with the Awanui Scarp in the center of the reentrant. The above observations suggest two models of reentrant formation. In the first, a subducted ridge may have dragged landward the tips of the rock slivers and created the reentrant by failure of the inner trench slope. In the second, the strike-slip component of the plate motion could have produced extension across a pre-existing transverse fault at the location of the N127°E trending wall by stretching and southwestward translation of block B rock slivers relative to block C. This extension forming a transverse extensional basin could, together with the proximity at the trench of a free boundary, have triggered both a northeastward and trenchward subsidence of the slivers of block B along the Awanui Fault (Figure 20). The lack of sliver deflection on the northern reentrant margin and the 30° difference between the direction of the northern reentrant wall and the PAC-TK convergence direction lead us to favoring the latter translation model.

The bathymetric low lying immediately southwest of block B forms a roughly rectangular, 10 km long by 5 km wide, flat-bottom trough that is 3250 m deep (Figure 4). The trough truncates the NE trending structures of block B along a N150°E, 600-m-high scarp and is bounded northwestward and southwestward by 1000-1200-m-high segments of the Awanui Fault scarp trending, N52° E and N150° E respectively. A 5-km left-step of the Awanui Fault immediately south of the trough makes the translation mechanism an unlikely model for this reentrant. We interpret the rectangular trough as a fault-bounded subsiding basin and suggest that its development relates to preexisting cross and strike faults. The faults

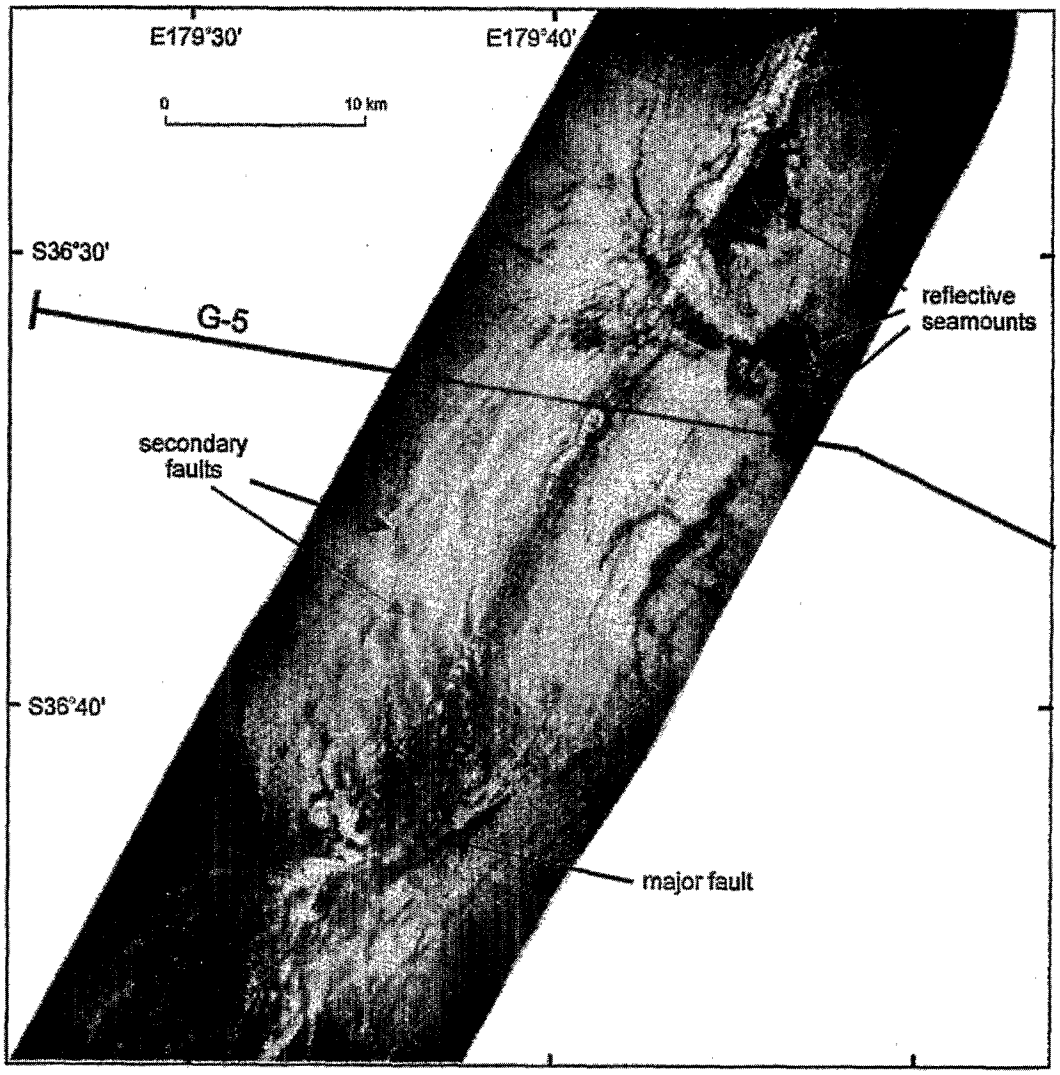

Figure 13. MR1 side-scan sonar imagery of a deformed zone at the transition between the forearc basin (west) and the East Cape Ridge (east); location and interpretation are shown in Figure 8.

oriented west or north-west across the margin have formed, parallel to the VMFZ [*Herzer and Mascle*, 1996] and the continental-oceanic boundary in the Bay of Plenty [*Wright*, 1993] during the structural development of the North Island northern margin, whereas the northeast trending faults (the Awanui Fault and ECR shear zone) have formed parallel to the Neogene strike-slip faults along the North Island [*Cutten*, 1994; *Delteil et al.*, 1996]. We suggest two possible models evolving from such intersecting fault trends: (1) the rectangular basin could have formed by trenchward collapse of the lower part of the inner trench wall bounded by the above faults or (2) the basin could have resulted from block rotation associated with dextral shearing between the upper and lower parts of the slope (Figure 21). The landward convexity of the arcuate structures of the southern part of block B together with the left-stepping of the Awanui Fault and N150°E-trending structural blocks of the middle part of the slope (Figure 8) provides support for the latter model which we prefer. Block rotation about a vertical axis requires a basal decoupling at depth, which could be achieved at the inter-plate décollement [*Nicholson et al.*, 1986]. The décollement beneath structural blocks of the middle slope is presently about 8-10 km deep. Vertical dimensions of rotated blocks are expected to be greater or similar to the horizontal dimensions. With sides 15-20 km wide, structural blocks of the middle slope may have been much thicker and farther from the deformation front when it originally formed. A significant amount of block rotation can be achieved only if lateral displacement of rocks is allowed. *Delteil et al.* [1996] showed that up to 300 km of cumulated displacement may have occurred onshore during the Miocene. Block rotation creates space problems that can be accommodated by relative vertical movements [*Schreurs*, 1994] thus accounting for the subsidence of the basin between rotated blocks and rocks of the adjacent lower margin.

6. Discussion

6.1. Nature and Origin of the East Cape Ridge

The ECR coincides with ~50-mGal-high free-air gravity anomalies (Figure 1), and discrete magnetic anomalies extend

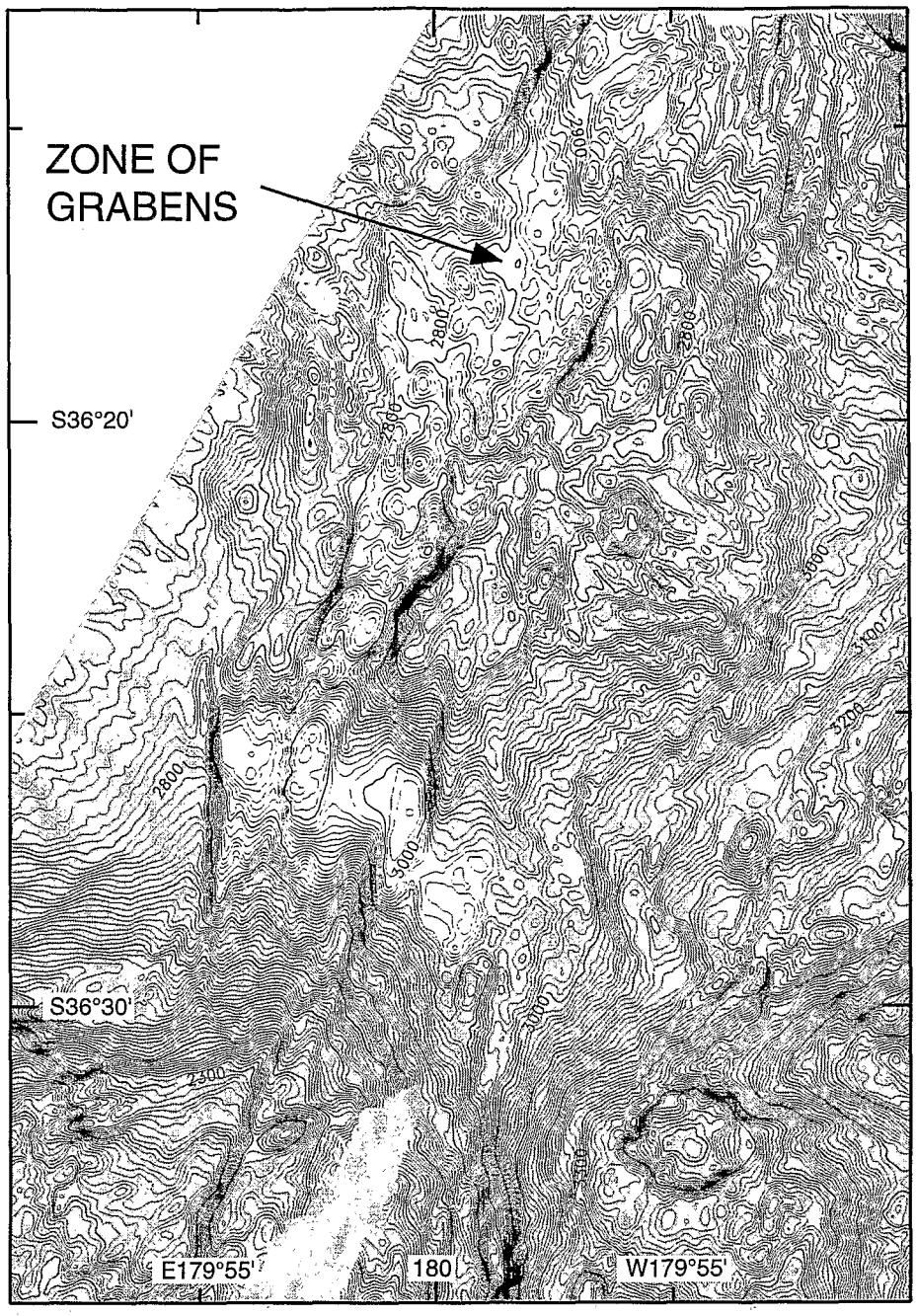

Figure 14. Detailed bathymetric map of the East Cape Ridge summit showing graben structures; contours every 10 m; location and interpretation are shown in Figure 8.

along its western flank (Figure 16). These anomalies are associated with crustal rocks of high magnetization and density [*Gillies*, 1984]. *Gillies and Davey* [1986] also measured compressional velocities of 5.4-7.4 km/s at depth greater than 5 km beneath the ridge and adjacent forearc basin. These velocities, although derived from unreversed refraction profiles, are comparable with crustal velocities of the Tongan platform and forearc [*Pontoise et al.*, 1980] and suggest that the ECR and Raukumara basin could be floored by island arc crust. This crust appears to be bounded seaward by the Awanui Fault, which we interpret as a landward dipping, reverse fault that has accommodated strike-slip deformation. The sharp contrast across the fault between the relatively little deformed basement of the middle margin and the strongly imbricated lower margin suggests that the island arc crust behaves as a core buttress or basement backstop [*von Huene and Scholl*, 1991] against which rests the lower slope accretionary wedge.

We speculate that the basement of the ECR and forearc basin could be the southernmost extension of the Eocene-Miocene Tonga volcanic arc. Geosat gravity data [*Sandwell and Smith* , 1994] indicate that the Tonga Platform extends along the eastern flank of the Kermadec Ridge as far south as 31°S, where the platform is truncated at the trench (Figures 1 and 22). From 31°S to 34°S the Kermadec forearc slope is steep

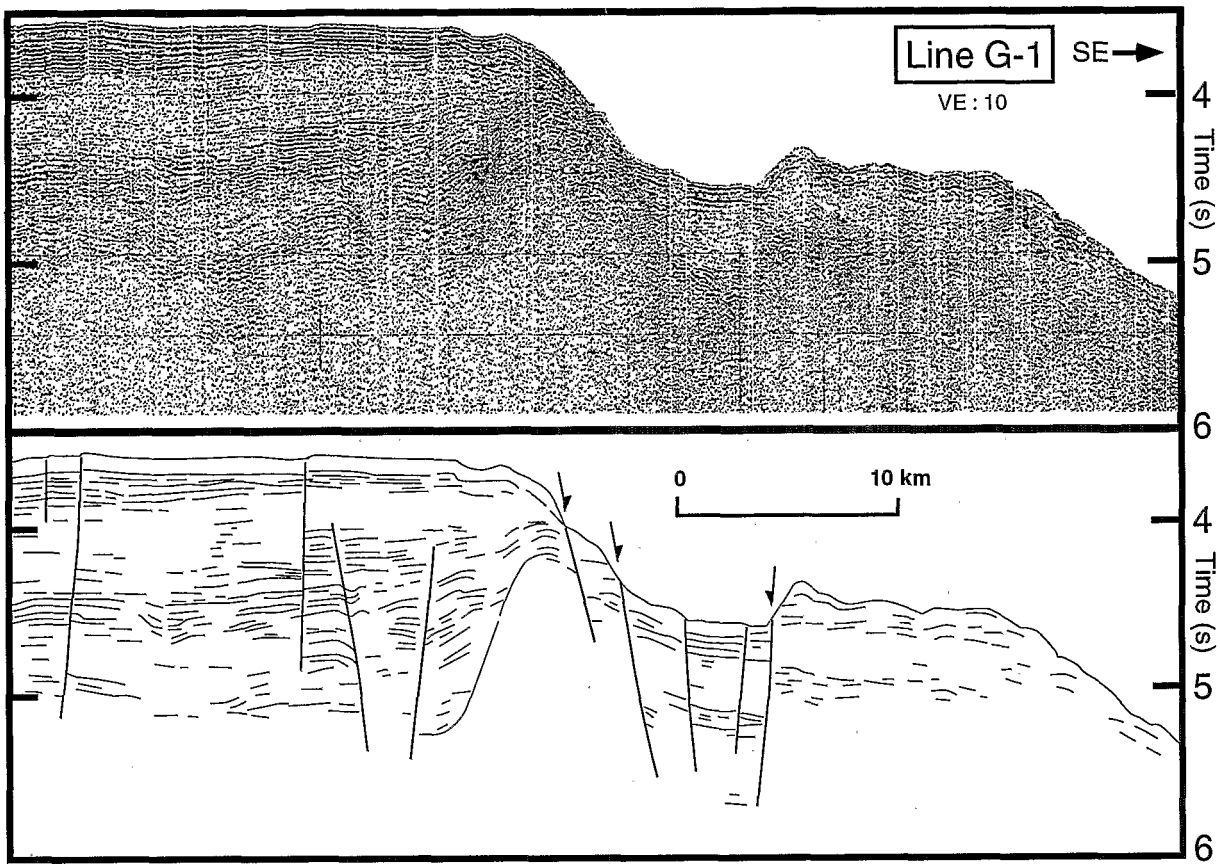

Figure 15. Seismic reflection line G-1 with line drawing; location is shown in Figure 2.

and shows extensional deformation [*Pelletier and Dupont*, 1990b], and the trench is offset arcward by about 20 km. South of 34°S, the Raukumara Basin develops southward along the seaward side of the Kermadec arc. We suggest that the Tonga Platform once extended continuously along of the Kermadec Ridge but has been tectonically eroded between 31°S and 35-36°S by the oblique subduction of the Hikurangi Plateau. This process may have been enhanced by southward transfer of Tongan forearc slivers along strike-slip faults because convergence obliquity was relatively high prior to the Pliocene. In this hypothesis, a deformed segment of the ancient Tonga arc would be preserved beneath the Raukumara basin and East Cape Ridge because they both presently override the subducting part of the plateau. However, because of basal tectonic erosion and the ongoing southward sweep of the Hikurangi Plateau along the trench, in the wake of the Rapuhia Scarp transit, the ECR and associated forearc basin subside northward, and the lower trench slope collapses into the trench. The collapse products in the trench are subsequently subducted. In this scenario, assuming a constant strike of the Rapuhia Scarp of N145°E (the major uncertainty) and a 6 cm/yr southward migration rate of the scarp-trench intersection based on the present-day plate convergence vector, the initial collision of the Hikurangi Plateau would have occurred at 31°S about 10 Myr ago.

6.2. Nature and Tectonic Evolution of the Inner Trench Slope Structures

With the existing limited seismic reflection coverage we must assume that the seismically reflective, imbricated sedimentary wedge shown on seismic line Explo-1 (Figure 7) is typical of the overall nature of the lower inner trench slope structures. Seafloor morphology suggests, however, that basement slivers may be a more significant feature of the lower slope to the north of the Explo-1 line.

The lower inner trench slope can be interpreted to consist of a transpressively deformed non growing accretionary wedge with a narrow and discontinuous fold-and-thrust belt at the toe of the slope. This structure and the distribution of the belt along the trench suggest that the products of mass wasting that pond locally into slope reentrants are imbricated and accreted together with some pelagic sediment scraped off the Hikurangi Plateau. The small size of the belt is attributable to the lack of trench fill and the bulldozing effect of normal faults on the plateau that are relatively high with respect to the size of the belt. We suggest that the belt grows seaward on narrow flat segments of the Hikurangi Plateau until the belt reaches a landward facing normal fault scarp on the plateau (Figures 11 and 20). At this stage, thrust sheets start to deform internally and stack against the scarp until a shape of least resistance is formed in a similar manner to that predicted in front of subducting seamounts [*Lallemand et al.*, 1994]. The décollement then moves to the surface of the stacked thrust sheets, which are subsequently subducted. Such a process accounts for the low, present-day, tectonic accretion budget.

Tectonic erosion has shaped inner trench slope structures as well. Transpressive rock slivers, oblique to the margin, and comprising most of the inner trench accretionary wedge extend to within a few kilometers of the accretionary front north of 36°30'S, where they are tectonically truncated. In

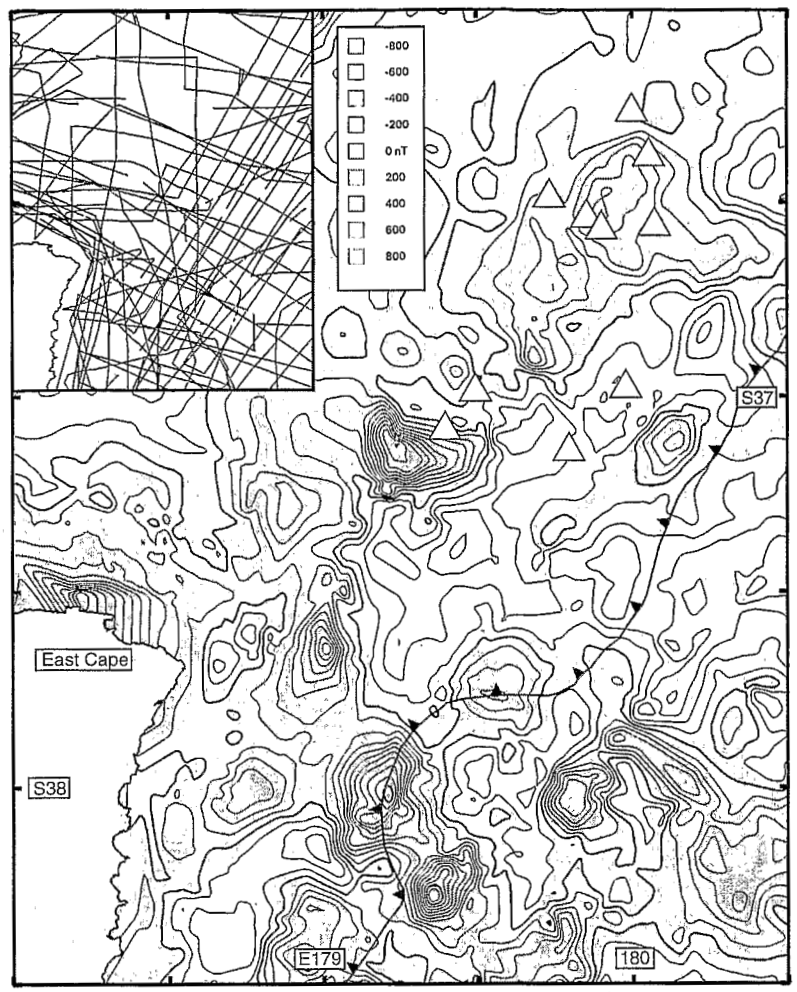

Figure 16. Magnetic anomaly map of the southern East Cape Ridge. The tracks of magnetic data are shown in the inset. Anomaly contours are every 50 nT. Open triangles mark highly reflective seamounts also shown by stars in Figure 8.

addition to the sliver truncation, the lack of growth due to tectonic accretion, the seaward collapse and mass wasting of the margin, and the lateral transport of the wedge rocks associated with strike-slip faulting all act to narrow, as is increasingly observed northwards, the width of the South Kermadec accretionary wedge.

The wedge has been constructed against an island arc backstop, which includes the upper and middle slope regions of the South Kermadec margin and appears, particularly south of 36°40'S, to be deforming by transpressional deformation. This deforming backstop shows a similarity (including a backstop thrust, the Awanui Fault, and a backstop transcurrent fault zone, the ECR shear zone) in structure and position to the backstop thrust and sheared zone of outer margin highs in the obliquely convergent central Aleutian margin [*Ryan and Scholl*, 1989]. The Kermadec ECR sheared zone appears wider (60 km versus 15 km) than the corresponding central Aleutian sheared zone. In addition to deforming the backstop, transcurrent faulting has significantly deformed the South Kermadec accretionary wedge. Similar faulting is reported in the eastern Aleutian accretionary wedge [*Lewis et al.*, 1988] although the morphologic expression of strike-slip faulting and associated structures in this wedge are less well expressed than along the South Kermadec margin.

The width and degree of strike-slip deformation at convergent margins depend on the intensity of interplate coupling relative to the strength of the margin material, combined with the obliquity of convergence. For the South Kermadec margin, we expect a greater degree of interplate coupling than for typical accretionary margins where oceanic crust is being subducted, such as in the Aleutian margin. The greater degree of interplate coupling is due to the buoyancy of the subducting Hikurangi Plateau crust and the enhanced basal friction. The Hikurangi Plateau buoyancy increases the contact pressure across the interplate interface, which in turn increases the basal friction. Basal friction also increases as a function of the ruggedness of the plateau. The Hikurangi Plateau also has a higher angle of obliquity (40° before 5 Ma) than the Aleutian margin, thus favoring strike-slip deformation.

The time of wedge development east of the Awanui Fault is poorly constrained within the ~40 Myr history of the Kermadec-North Island margin [*Walcott*, 1987]. However, the structural complexity of the inner trench slope favors a multiphase tectonic development that may have initiated prior

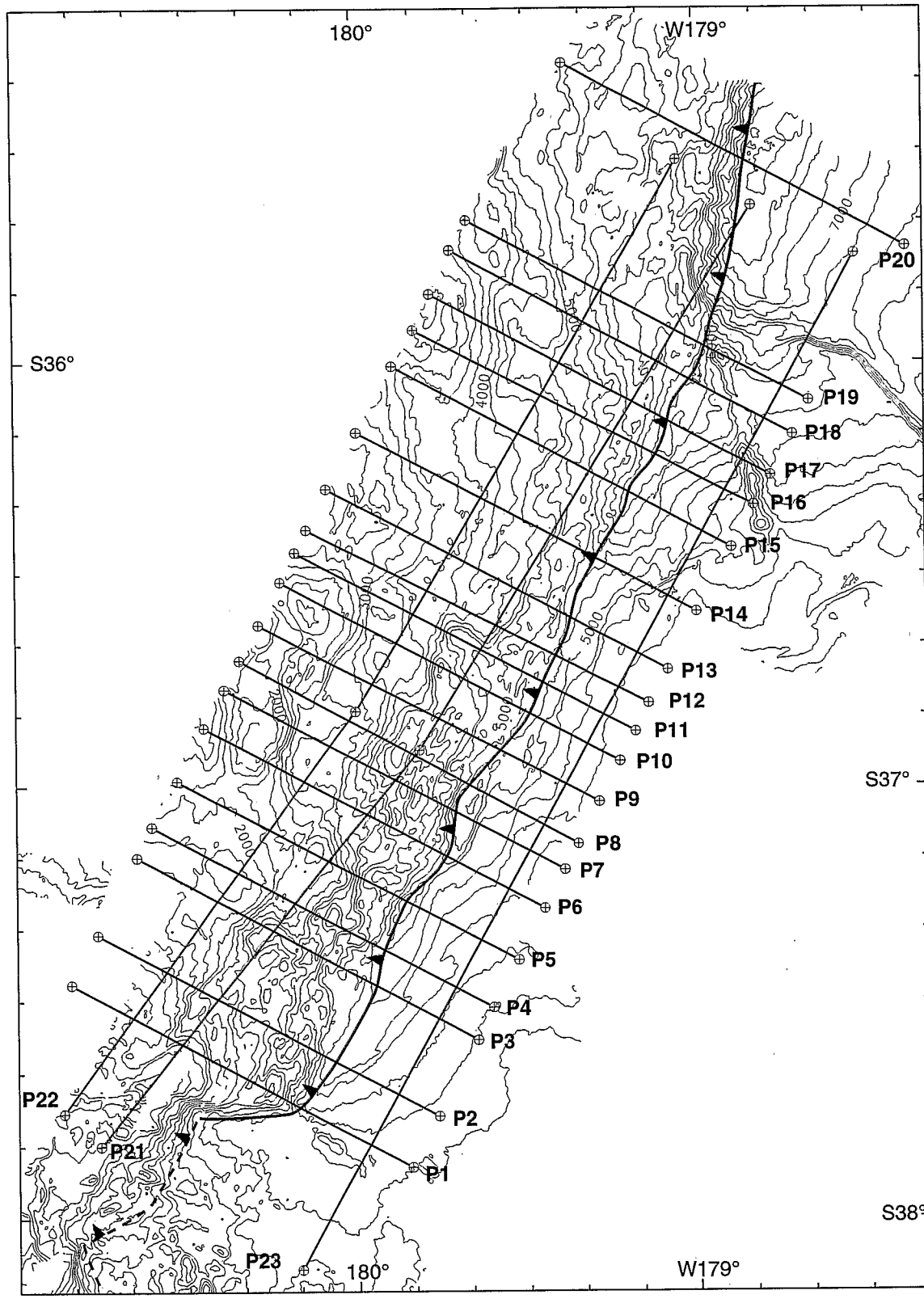

Figure 17. Location of bathymetric cross-sections shown in Figures 18 and 19.

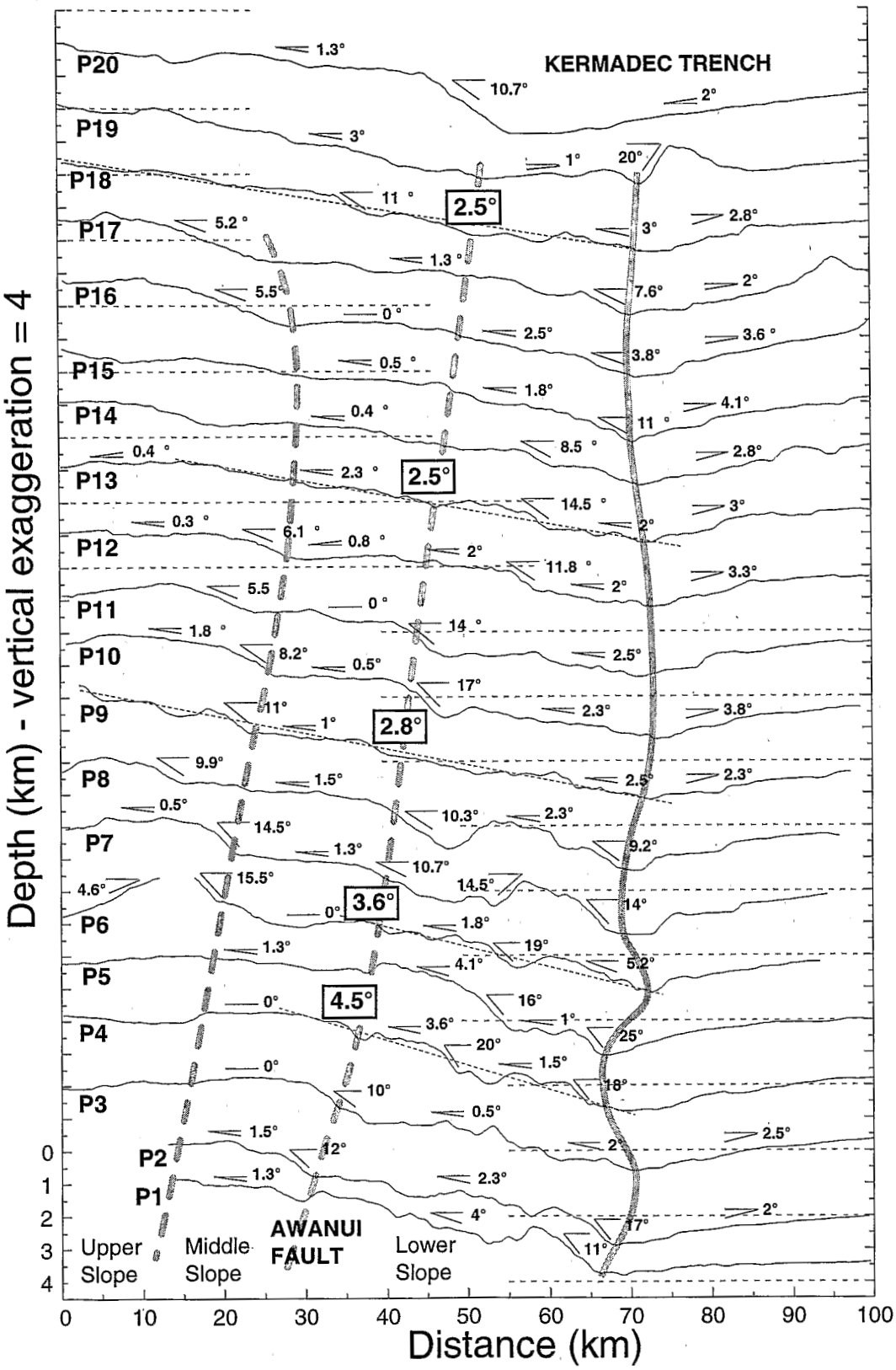

Figure 18. Selected bathymetric sections across the South Kermadec Trench/ Hikurangi Plateau subduction zone with slope values in degrees. These sections are extracted from the gridded bathymetry, in a direction perpendicular to the trench. The horizontal dashed lines indicate the 3000 m depth. Note that the average angle of the inner trench slope (bold numbers in boxes) decreases northward, the middle slope remains subhorizontal, and the lower slope shows drastic changes in dip angle (0.5° to 20°). The toe of the lower slope dips locally at a small (2°) angle that is consistent with imbricated structures. This lower slope dips landward on section P19, where a ridge is being subducted; Sections are located in Figure 17.

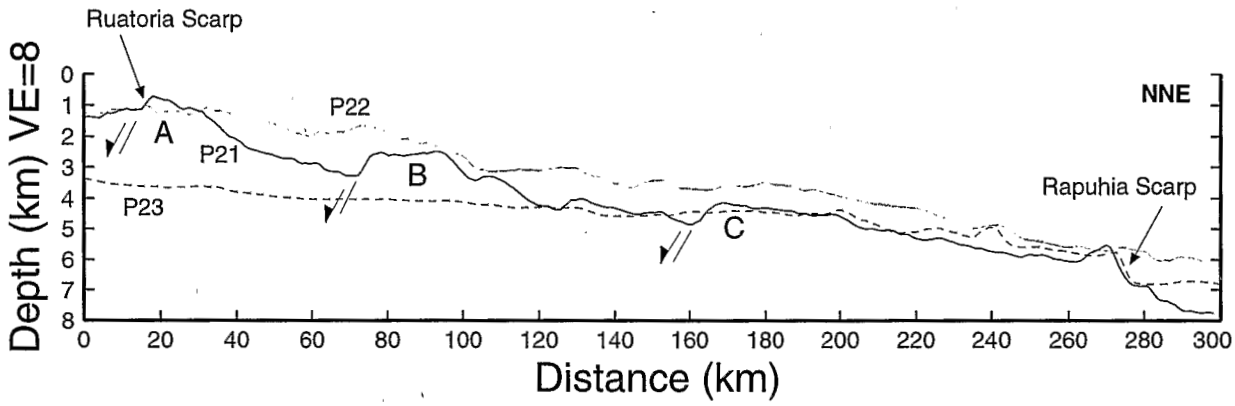

Figure 19. Along-strike bathymetric sections of the lower slope (thick line), middle slope (thin line) of the South Kermadec Trench and the Hikurangi Plateau (dashed line); note that the Hikurangi Plateau dips north and that the lower slope shows major vertical offsets that separate slope segments tilted northward; A, B, and C are structural blocks described in text; location of sections is shown in Figure 17.

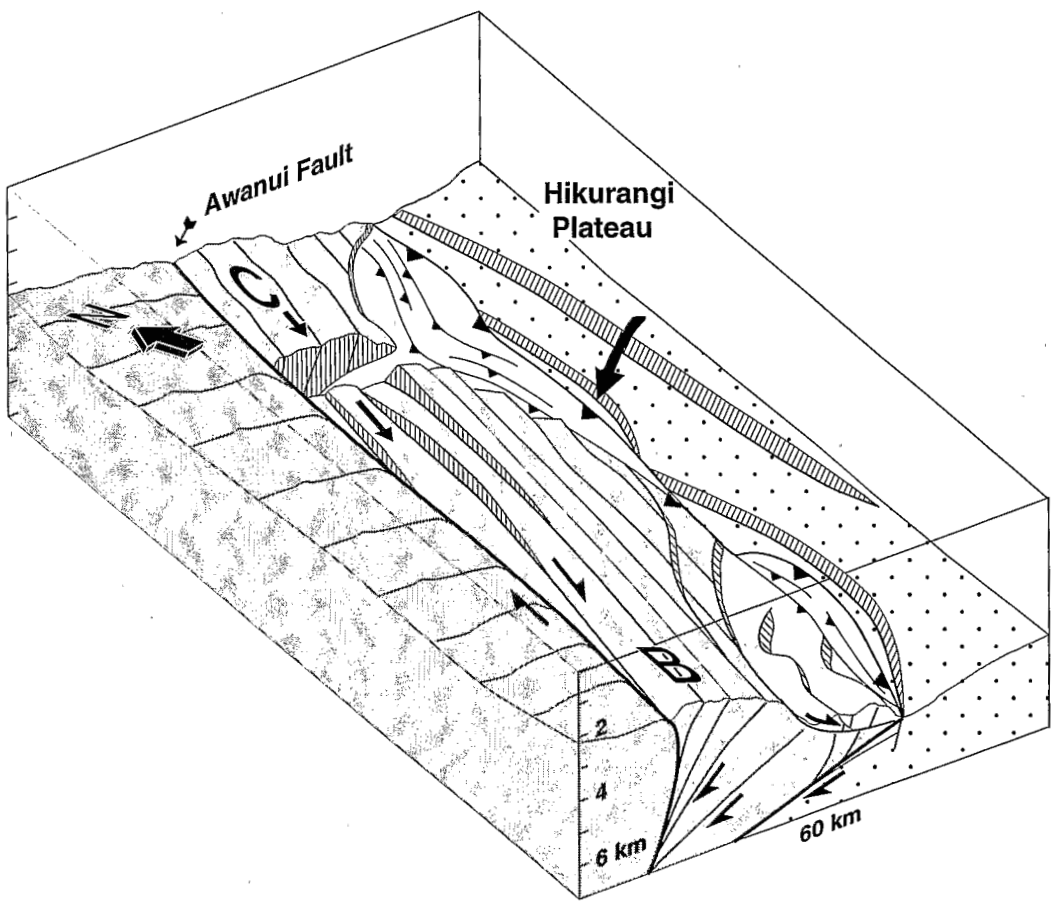

Figure 20. 3D-structural sketch of the lower and middle parts of the southern (36°30'S to 37°15'S) Kermadec inner trench wall. Accreted rocks (middle shading) form slivers transpressively deformed against the backstop (dark shading) along the Awanui Fault. B and C are structural blocks described in text. Owing to differential stretching, related to lateral transport, rock slivers ruptured transversally and subsided to form the deep reentrant. Frontal areas of collapse and truncation of the slivers (light shading) are represented as well as limited zones of tectonic accretion (white zones bounded by teeth).

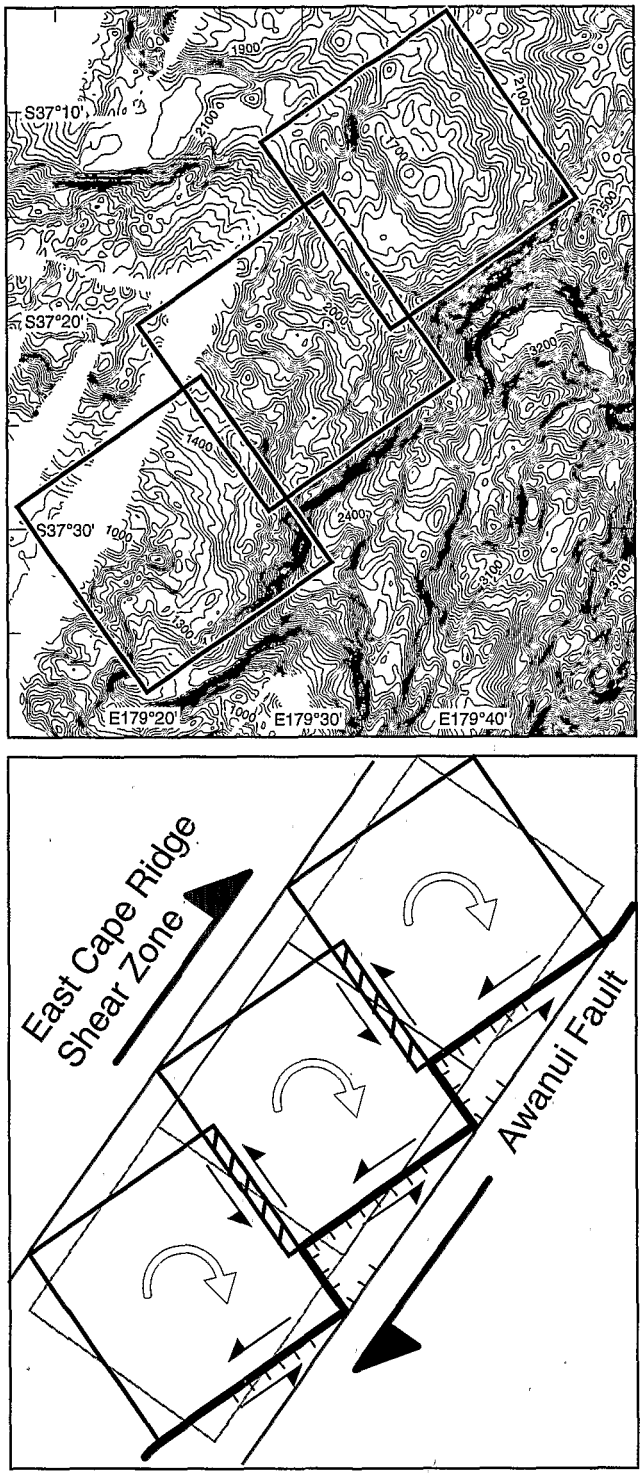

Figure 21. (top) Detailed bathymetric map of the southern part of the South Kermadec Trench showing interpreted rotated blocks; contours every 25 m. (bottom) Sketch of rotated block mechanics showing a possible mechanism for the basin formation. Areas of compression (striped) and extension (hatched edges) are marked.

to the subduction of the Hikurangi plateau. Rock slivers of the wedge appear, based upon their linearity and oblique angle to the backstop, to have been accreted obliquely and later deformed by dextral transpression along the Awanui Fault as indicated by block rotation and rock sliver translation that postdates tectonic accretion. The accretionary ridges lack intervening piggy-back basins of classical, low basal friction accretionary wedges and are bounded by steeply dipping reverse faults (Figure 20) suggesting a relatively strong basal friction and a high degree of compression against the backstop, possibly during initial subduction of the Hikurangi Plateau. The multiphase tectonic development of the margin suggests that preexisting structural discontinuities, such as the seaward edge of the backstop, and early faults like the reverse and thrust faults formed in the accretionary wedge were reactivated with a strike-slip component to form respectively the Awanui Fault and most of the sliver bounding strike-slip faults. A consequence of complex faulting related to oblique subduction of the plateau is to diminish the global strength of the wedge. However, in order to transmit the stresses necessary to reactivate or create the sliver bounding strike-slip faults, the slivers must have formed in moderately rigid rocks at a considerably greater distance from the accretionary front than at present, consistent with our interpretation of an eroding, narrowing margin.

Strike-slip motion is still active in the wedge as suggested by the small dextral lateral offsets documented across the Ruatoria Scarp at the southern termination of the wedge. Evidence of active thrusting and folding from the Explo-1 and MOB-131 lines indicates that the wedge also deforms internally by compression in order to maintain its critical taper as discussed in section 6.3.

6.3. Present-Day Tectonic Regimes, Slope Stability and Internal Parameters of the Wedge

The analysis of the tectonic regimes of the inner trench wall combined with an examination of its mechanical stability in terms of a Coulomb wedge can be used to address some of the internal parameters of the wedge. *Davis et al.* [1983] have shown that a sedimentary accretionary wedge can be modeled as noncohesive frictional material or Coulomb material. Such a wedge, when compressed horizontally on a weak basal plane, will deform internally until it reaches a "critical taper" defined as its topographic slope (α) added to the dip of its basal décollement (β). This critical taper at failure depends on characteristic parameters: the internal and basal friction coefficients (μ, μ_b) and pore fluid pressure ratios (λ and λ_b) of the wedge. The basic parameters can be reduced to three (μ, μ^*_b, and λ), inasmuch as the effective basal friction μ^*_b is a function of μ_b, λ, and λ_b.

Lallemand et al. [1994] proposed a mean stability field diagram (α versus β, Figure 23), that they constructed from mean measured parameters (μ, μ^*_b, λ in Figure 23) to separate three categories of convergent margin. Actively growing accretionary wedges have low taper (5°) and fall in the unstable compressional area of the diagram; the intermediate accretionary wedges are located in the mean stability field or in the vicinity of the upper extensional envelope, and the nonaccretionary wedges, which have high taper (16-20°) are mainly in the extensional domain. The mean α calculated across the South Kermadec inner trench wall ranges from 4.5° to 2.5° (Figure 18), and a 5.5° mean β can be estimated from both a 3-4° dip angle of the outer trench wall and a 7-8° dip of the Benioff zone beneath the East Cape Ridge. These data provide an average taper of 8° to 10°, suggesting that the South Kermadec margin is an intermediate accretionary wedge, which should therefore be stable or deform by extension.

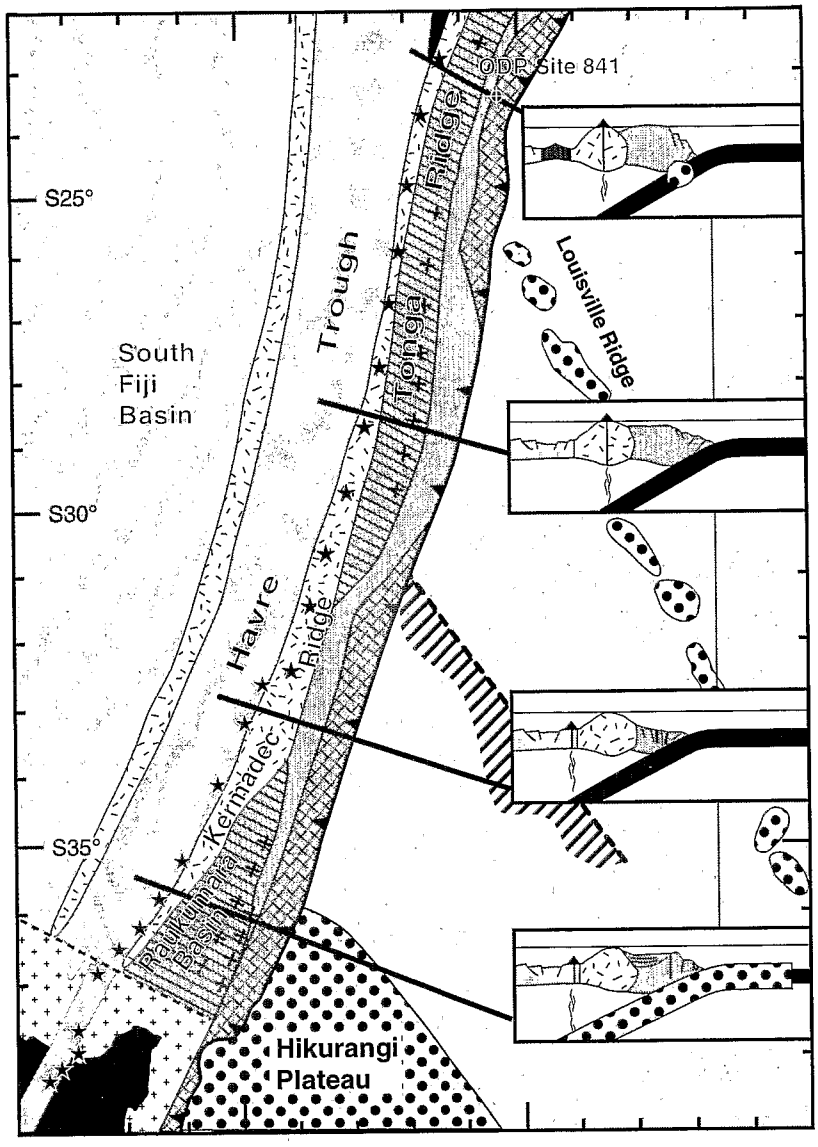

Figure 22. Structural interpretation of the Tonga-Kermadec forearc based on Geosat gravity data and bathymetric data. Cross sections of the subduction zone illustrate the westward shift of the volcanic line near 32°S and the relatively increased tectonic erosion of the Tonga platform (cross-hatched area) associated with the southward sweep of the Louisville Ridge in the north and Hikurangi Plateau in the south. The best preserved segment of the Tonga forearc lies between 27° and 31°S. Note the approximate geographic correlation between the interpreted area of initial impact of the Hikurangi Plateau (dashed line with striped area on downgoing plate) where the southern tip of the Tonga Platform is truncated and the westward shift of the volcanic line (near 32°S). Tectonic erosion [*Lallemand*, 1995] and a decrease in the dip of the Benioff Zone associated with the subduction of the buoyant Hikurangi Plateau relative to the surrounding oceanic crust are believed to be the cause of the westward shift in the volcanic line and the associated landward retreat of the trench.

However, most geophysical data presented in this paper indicate that the wedge is deforming internally under transverse compression, although a strike-slip component has been influencing its structural development. Strike-slip tectonics produce high-angle (subvertical) faults that favor local slope instabilities and variations in rock lithology by longitudinal transfer of basement rocks or indurated sediment against accreted sediment. At a smaller scale, the lower part of the wedge shows large slope variations (up to 20°, Figure 18) indicating either a change in rock lithology, local slope instabilities of tectonic origin, or local changes of the characteristic parameters such as the basal friction.

Comprehensive evidence for gravitational collapse and mass wasting suggests that parts of the lower inner trench wall are affected by tectonic erosion. We thus infer that the dominant compression and associated substantial collapse within an 8-10° wedge taper reflects a strongly reduced stability field. *Lallemand* [1992] has shown that for a given average friction, if the pore fluid pressure is low ($\lambda = 0.55$), the stability field envelope is large and the wedge can sustain slopes ~20°. Conversely, if the fluid pressure is high ($\lambda = 0.97$), the stability envelope is reduced and the topographic slope of the wedge will only be stable for slope angles less than 2° [*Lallemand et al.*, 1994]. Following this rational, a

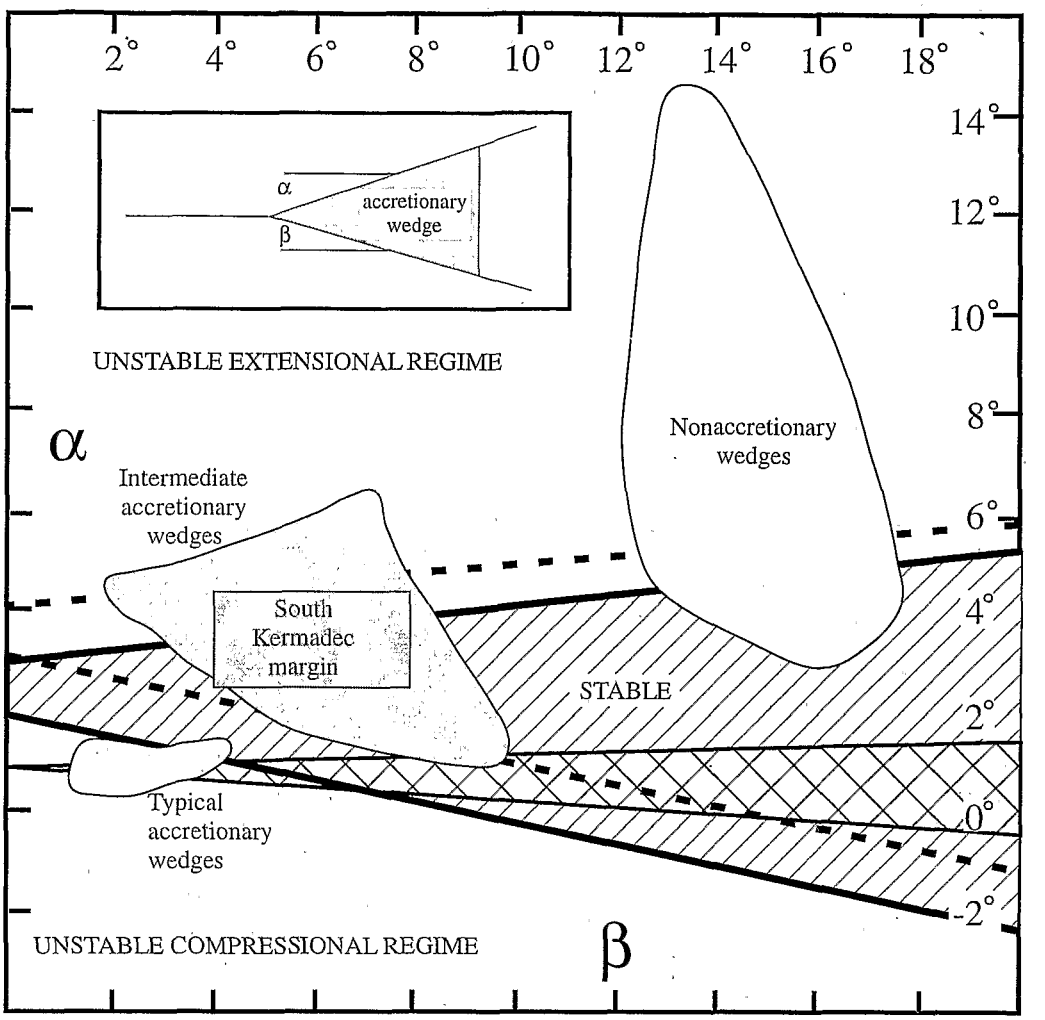

Figure 23. Characteristic Coulomb wedge stability envelope (stippled area) obtained using mean measured friction coefficients (μ =0.52, μ^*_b =0.24) and pore fluid pressure ration λ =0.88 [after *Lallemand et al.*, 1994] (surface slope α versus basal dip β). The position of the South Kermadec margin (α = 3.5°, β = 5.5°) is marked with other typical types of wedge. In order to realize the observed compressionally unstable nature of the South Kermadec margin, the stability envelope must be reduced and lie at higher α than the characteristic envelope. This can be achieved by increasing the pore pressure (cross-hatched area, λ =0.97) and increasing effective basal friction (dashed envelope, μ^*_b =0.34) over values assigned to an average margin.

smaller stability field can be achieved by increasing λ. Moreover, although the stability field is not very sensitive to variations of the internal friction (μ,), an increased effective basal friction (μ^*_b) would tend to move the stability envelop toward higher α, thus allowing compression to occur for steeper topographic slopes. Hence relatively high λ and μ^*_b are expected in the South Kermadec wedge and are supported by the absence of trench fill turbidite, the lack of a growing accretionary wedge and the ruggedness of the Hikurangi Plateau. Indeed, in nongrowing accretionary wedges, shallow trench sediments, which have a higher fluid content than underlying sediments, are subducted and subsequently dewatered at depth beneath the wedge [*Le Pichon et al.*, 1990]. If the convergence rate is faster than the dewatering rate, overpressured fluids would favor basal tectonic erosion by hydrofracturation [*Von Huene and Scholl*, 1991; *Lallemand et al.*, 1994]. The South Kermadec wedge is highly faulted and allows fluids entrained with subducted sediment to escape from the décollement and diffuse into the wedge raising the internal pore pressure.

The variation from transpression to extension along the ECR (Figure 8) reveals the complex interplay between underplating, erosional processes, subducting plate dip changes, and ruggedness in the surface of the subducting plateau. A relatively strong basal friction is attributed to fault scarps and volcanic ridges, enhancing the ruggedness of the outer trench wall, although the subduction of hemipelagic sediments would tend to reduce μ^*_b. The transpressive zone indicates increased coupling between the elevated southern part of the plateau and the northern corner of North Island continental crust. Extension at the ECR summit may result either (1) from uplift as a consequence of sediment underplating or subduction of a high region of the plateau, or (2) from a trenchward tilt of the margin associated with basal erosion of the lower slope. There are grabens located at 36°-36°40'S, on the ridge summit, as well as grabens that are tilted

trenchward north of 36° S where the ECR is deeper. The general models of seamount subduction developed by *Lallemand and Le Pichon*, [1987] and *Von Huene and Lallemand*, [1990] suggest that subduction of a NNW trending, high region of the plateau could account for the distribution of deformation. Such a high underthrusting of the ECR at 36°20'-36°40'S, would uplift this region, producing superficial extension. Because of the oblique convergence, the high would transpressively deform the southern part of ECR as upper plate rocks ride up the western flank of the high. Once upper plate rocks passed the summit of the subducting high and started traveling down its trailing flank, subsidence of the inner trench slope would occur as well as trenchward tilt of the grabens that formed above the high. Alternatively, basal erosion of the lower part of the margin could lead to extension along the ECR by producing a trenchward tilt of the margin. Increased tectonic erosion in the northern part of the survey associated with higher and more abundant normal faults on the outer trench wall, compared with farther south, would force the trench to retreat landward and the inner trench slope along with the grabens to collapse trenchward. This process should logically increase the dip of the trench inner slope in the north. The dip, however, is smaller in the north (2.5°) than in the south (4.5°), suggesting that the subduction of a high region of the Hikurangi Plateau is the more likely dominant factor behind the ridge crest extension despite the absence of an observed corresponding ridge on the Hikurangi Plateau east of the trench, or any indication of such a structure in the magnetic anomaly data (Figure 16).

7. Conclusions

The geophysical data presented above indicate that the South Kermadec margin consists of a deforming and subsiding island arc crust against which an accretionary wedge was emplaced during oblique convergence. The existence of this presently nongrowing wedge indicates that the sedimentologic conditions changed drastically from a sedimented paleo-Kermadec Trench to a sediment-starved trench.

The wedge, as well as the backstop, were subsequently deformed by transpression, block rotation, sliver translation, normal faulting and tectonic erosion. These tectonic processes result from a relatively increased interplate coupling associated with the oblique subduction of the Hikurangi Plateau. Subduction of the Hikurangi Plateau is inferred, because of its greater buoyancy than normal oceanic crust, to be only marginally favored dynamically [*Davy* 1992, *Cloos* 1993]. The increased interplate pressure relative to that produced by a heavier normal oceanic crust together with the surface ruggedness of the plateau increase the interplate coupling. The compressional nature of the margin, comparatively modest taper of ~8-10° and evidence of mass wasting suggest that much of the margin is unstable under compression due to internal elevated pore pressures but high basal friction on the décollement.

The crest of the ECR, as well as showing evidence of transpressive faulting which accommodates some of the oblique motion at the margin, also exhibits graben extension north of 36°40'S inferred to result from uplift of the ECR. This uplift may be associated with subducted Hikurangi Plateau topography or underplating of sediment eroded from the leading edge of the margin. Subsidence of the ECR crest north of 36° S is presumed to relate to the similarly northward deepening Hikurangi Plateau and proximal plateau margin (the Rapuhia Scarp) being subducted beneath the southern Kermadec margin in this region.

Subsidence and tectonic erosion of the upper margin in the wake of the Hikurangi Plateau are inferred from the seismic reflection, gravity, and bathymetry data. North of 31°S the corresponding upper margin component of the Tonga Ridge is still recognized in the gravity data, indicating it has not been subject to collapse following Hikurangi Plateau collision. This suggests that the East Cape Ridge is a section of the Tonga Ridge which will subside following the southward sweep of the subducting Rapuhia Scarp, in a manner similar to the section between 36° and 31°S.

Acknowledgments. We are grateful to the New Zealand Foundation for Research Science and Technology (FRST), the Institute of Geological and Nuclear Sciences (IGNS), l' Institut Français de Recherche Scientifique pour le Développement en Coopération (ORSTOM) for funding and IFREMER for providing ship time, equipment, and Trismus software that we used to process swath data. We thank the National Institute of Water and Atmospheric Research (NIWA) and Seabed Mapping New Zealand Ltd. for providing MR1 swath data, F. Davey for supplying MCS line Explora, the scientific party of the GEODYNZ-SUD cruise Leg 1 for discussions, as well as G. Lamarche for help in seismic and bathymetric processing. We would like to thank F. Davey, S. Lallemand, and H. Ryan for helpful suggestions and critical reviews to improve the manuscript. C. Hume assisted with figure production. This work is contribution 143 of the UMR-6526 Géosciences Azur CNRS-ORSTOM-UPMC-UNSA and IGNS project 546310.

References

Anderson, H., E. Smith, and R. Robinson, Normal faulting in a back-arc basin: seismological characteristics of the March 2, 1987, Edgecumbe, New Zealand, earthquake, *J. Geophys. Res.*, *95*, 4709-4725, 1995.

Ballance, P. F., Evolution of the Upper Cenozoic magmatic arc and plate boundary in northern New Zealand, *Earth Planet. Sci. Lett.*, *28*, 356-370, 1976.

Ballance, P. F., The New Zealand Neogene forearc basins, in *South Pacific Sedimentary Basins*, edited by P. F. Ballance, pp. 177-193, Elsevier Sci., New York, 1993.

Ballance, P. D., D. W. Scholl, T. L. Vallier, A. J. Stevenson, H. Ryan, and R. H. Herzer, Collision effects of Louisville Ridge, subduction of a Late Cretaceous seamount of the Louisville ridge at the Tonga Trench: A model of normal and accelerated tectonic erosion, *Tectonics*, *8*, 953-962, 1989.

Bloomer, S. H., A. Ewart, J. M. Hergt, and W. B. Bryan, Geochemistry and origin of igneous rocks from the outer Tonga forearc (Site 841), *Proc. Ocean Drill Program, Sci Results*, *135*, 625-646, 1994.

Cadet, J.-P., et al., The Japan trench and its juncture with the Kurile trench: Cruise results of the Kaiko project, Leg 3, *Earth Planet. Sci. Lett.*, *83*, 267-284, 1987.

Cloos, M., Lithospheric buoyancy and collisional orogenesis: Subduction of oceanic plateaus, continental margins, island arcs, spreading ridges, and seamounts, *Geol. Soc. Am. Bull.*, *105*, 715-737, 1993.

Cole, J. W., Distribution and tectonic setting of Late Cenozoic volcanism in New Zealand, *R. Soc. N. Z. Bull.*, *23*, 7-20, 1986.

Collot, J.-Y., and M. A. Fisher, The collision zone between the North d'Entrecasteaux Ridge and the New Hebrides Island Arc, 1, Sea Beam morphology and shallow structures, *J. Geophys. Res.*, *96*, 4457-4478, 1991.

Collot, J.-Y., et al., From oblique subduction to intra-continental transpression: structures of the southern Kermadec-Hikurangi margin from multibeam bathymetry, side-scan sonar and seismic reflection, *Mar. Geophys. Res.*, *18*, 357-381, 1996.

Corrigan, J., P. Mann, and J. C. Ingle, Forearc response to subduction of the Cocos Ridge, Panama-Costa Rica, *Geol. Soc. Am. Bull.*, *102*, 628-652, 1990.

Cutten, H. N. C., Geology of the middle Reaches of the Mohaka River, *Geol Map 6*, Sheet V19BD, scale 1:50,000, Inst. of Geol. and Nucl. Sci. Ltd., Lower Hutt, New Zealand, 1994.

Davey, F. J., S. Henry, and E. Lodolo, A seismic crustal section across the East Cape convergent margin, New Zealand, *Tectonophysics, 269*, 199-215, 1997.

Davis, D., J. Suppe, and F. A. Dahlen, Mechanics of fold-and-thrust belts and accretionary wedges, *J. Geophys. Res., 88*, 1153-1172, 1983.

Davy, B. W., The influence of subducting plate buoyancy on subduction of the Hikurangi-Chatham Plateau beneath North Island, New Zealand, in *Geology and Geophysics of Continental Margins*, edited by J. S. Watkins, F. Zhiqiang, and K. J. McMillen, AAPG Mem., 53, 75-91, 1992.

Davy, B. W., and R. Wood, Gravity and magnetic modeling of the Hikurangi Plateau, *Mar. Geol., 118*, 139-151, 1994.

Delteil, J., H. E. G. Morgans, J. I. Raine, B. D. Field, and H. N. Cutten, Early Miocene thin-skinned tectonics and wrench faulting in the Pongaroa district, Hikurangi margin, North Island, New Zealand, *N. Z. J. Geol. Geophys., 39*, 271-282, 1996.

de Mets, C., R. G. Gordon, D. F. Argus, and S. Stein, Current plate motions, *Geophys. J. Int., 101*, 425-478, 1990.

Dupont, J., Morphologie et structures superficielles de l'arc insulaire des Tonga-Kermadec, in *Contribution à l'Etude Géodynamique du Sud-Ouest Pacifique, Equipe Géologie-Géophysique Nouméa*, pp. 262-283, ORSTOM, Paris, 1982.

Fisher, M. A., J.-Y. Collot, and E. L. Geist, The collision zone between the North d'Entrecasteaux Ridge and the New Hebrides Island Arc, 2, structures from multichannel seismic data, *J. Geophys. Res., 96*, 4479-4495, 1991a.

Fisher, M. A., J. Y. Collot, and E. L. Geist, Structures of the collision zone between Bougainville Guyot and the accretionary wedge of the New Hebrides Island Arc, southwest Pacific, *Tectonics, 10*, 887-903, 1991b.

Fitch, T. J., Plate convergence, transcurrent faults, and internal deformation adjacent to Southeast Asia and the western Pacific, *J. Geophys. Res., 77*, 4432-4460, 1972.

Fryer, P., E. L. Ambos, and D. M. Hussong, Origin and emplacement of Mariana forearc seamounts, *Geology, 13*, 774-777, 1985.

Geist, E. L., M. A. Fisher, and D. W. Scholl, Large-scale deformation associated with ridge subduction, *Geophys. J. Int., 115*, 344-366, 1993.

Gillies, P. N., A marine geophysical study of the junction of the Kermadec and Hikurangi subduction systems, Ph.D. thesis, Univ. of Auckland, Auckland, New Zealand, 1984.

Gillies, P. N., and F. J. Davey, Seismic reflection and refraction studies of the Raukumara forearc basin, New Zealand, *N. Z. J. Geol. Geophys., 29*, 391-403, 1986.

Herzer, R. H., Seismic stratigraphy of a buried volcanic arc, Northland, New Zealand, and implications for Neogene subduction, *Mar. Pet. Geol., 12*, 511-531, 1995..

Herzer, R. H., and J. Mascle, Anatomy of a continent-backarc transform-The Vening Meinesz Fracture Zone northwest of New Zealand, *Mar. Geophys. Res., 18*, 401-427, 1996.

Houtz, R. E., J. Ewing, M. Ewing, and A. G. Leonardi, Seismic reflection profile of the New Zealand plateau, *J. Geophys. Res., 72*, 4713-4729, 1967.

Karig, D. E., Kermadec arc-New Zealand tectonic confluence, *N. Z. J. Geol. Geophys., 13*, 21-39, 1970.

Karig, D. E., and G. F. Sharman, Subduction and accretion trenches, *Geol. Soc. Am. Bull., 86*, 377-389, 1975.

Katz, H. R., Margins of the southwest Pacific, in *The Geology of Continental Margins*, edited by C. A. Burk and C. L. Drake, pp. 549-565, Springer-Verlag, New York, 1974.

Katz, H. R., Plate margin transition from oceanic arc-trench to continental system: The Kermadec-New Zealand example, *Tectonophysics, 87*, 49-64, 1982.

Kelleher, J., and W. McCann, Buoyant zones, Great earthquakes, and unstable boundaries of subduction, *J. Geophys. Res., 81*, 4885-4896, 1976.

Kibblewhite, A., C., Denham, R., N., The bathymetry and total magnetic field of the South Kermadec Ridge seamounts, *N. Z. J. Sci., 10(1)*, 52-67, 1967.

Kolarski, R. A., P. Mann, and W. Montero, Island arc response to shallow subduction of the Cocos Ridge, Costa Rica, *Spec. Pap. Geol. Soc. Am. Bull., 295*, 235-260, 1995.

Kroenke, L. W., Cenozoic tectonic development of the southwest Pacific, *U. N. CCOP/SOPAC Tech. Bull., 6*, 122, 1984.

Lallemand, S. E., High rates of arc consumption by subduction processes: some consequences, *Geology, 23*, 551-554, 1995.

Lallemand, S. E., Transferts de matière en zone de subduction, Mémoire d' habilitation à diriger des recherches, thesis, Uni. Pierre et Marie Curie, Paris VI, 1992.

Lallemand, S. E., and X. Le Pichon, Coulomb wedge model applied to subduction of seamounts in the Japan Trench, *Geology, 15*, 1065-1069, 1987.

Lallemand, S. E., P. S. Schnurle, and J. Malavieille, Coulomb theory applied to accretionary and non accretionary wedges: Possible causes for tectonic erosion and/or frontal accretion, *J. Geophys. Res., 99*, 12,033-12,055, 1994.

Lamb, S. H., Tectonic rotations about vertical axes during the last 4 Ma in part of the New Zealand plate-boundary zone, *J. Struct. Geol., 10*, 875-893, 1988.

Le Pichon, X., P. Henry, and S. Lallemant, Water flow in the Barbados accretionary complex, *J. Geophys. Res., 95*, 8945-8967, 1990.

Lewis, K. B., The 1500-km-long Hikurangi Channel: Trench-axis channel that escapes its trench, crosses a plateau, and feeds a fan drift, *GeoMarine Lett., 14*, 19-28, 1994.

Lewis, K. B., and D. J. Bennett, Structural patterns on the Hikurangi margin: an interpretation of new seismic data, in *New Seismic profiles, Cores and Dated Rocks From the Hikurangi Margin, New Zealand*, Oceanogr. Field Rep. 22, edited by K. B. Lewis, pp. 3-25, N. Z. Oceanogr. Inst., Wellington, New Zealand 1985.

Lewis, K. B., and J. R. Pettinga, The emerging, imbricate frontal wedge of the Hikurangi margin, in *South Pacific Sedimentary Basin*, edited by P. F. Ballance, pp. 225-250, Elsevier Sci., New York, 1993.

Lewis, S. D., J. W. Ladd, and T. R. Bruns, Structural development of an accretionary prism by thrust and strike-slip faulting: Shumagin region, Aleutian trench, *Geol. Soc. Am. Bull., 100*, 767-782, 1988.

McCaffrey, R., Oblique plate convergence, slip vectors, and forearc deformation, *J. Geophys. Res., 97*, 8905-8915, 1992.

McCann, W. R., and R. E. Habermann, Morphologic and geologic effects of subduction of bathymetric highs, *Pure Appl. Geophys., 129*, 41-69, 1989.

McGeary, S., A. Nur, and Z. Ben-Avraham, Spatial gaps in arc volcanism: the effect of collision or subduction of oceanic plateaus, *Tectonophysics, 119*, 195-221, 1985.

McLeod, C. J., Structure of the outer Tonga fore arc at Site 841, *Proc. Ocean Drill. Program, Sci. Results, 135*, 313-329, 1994.

Moretti, I., and K. Ngokwey, Aseismic ridge subduction and vertical motion of overriding plate, in *Caribbean Dynamics*, edited by A. Mascle, pp. 245-253, Technip, Paris, 1985.

Mortimer, N., and D. L. Parkinson, Hikurangi Plateau: A Cretaceous large igneous province in the southwest Pacific Ocean, *J. Geophys. Res., 101*, 687-696, 1996.

Nicholson, C., L. Seeber, P. Williams, and L. R. Sykes, Seismic evidence for conjugate slip and block rotation within the San Andreas fault system, southern California, *Tectonics, 5*, 629-648, 1986.

Orange, D. L., and M. B. Underwood, Patterns of thermal maturity as diagnostic criteria for interpretation of melanges, *Geology, 23*, 1144-1148, 1995.

Pelletier, B., and J. Dupont, Effets de la subduction de la ride de Louisville sur l'arc des Tonga-Kermadec, *Oceanol. Acta, vol. Spec. 10*, 57-76, 1990a.

Pelletier, B., and J. Dupont, Erosion, accretion, extension arrière-arc et longueur du plan de subduction le long de la marge active des Kermadec, Pacific Sud-Ouest, *C. R. Acad. Sci.*, ser. II, *310*, 1657-1664, 1990b.

Pelletier, B., and R. Louat, Seismotectonics and present-day relative plate motions in the Tonga-Lau and Kermadec-Havre region, *Tectonophysics, 165*, 237-250, 1989.

Pontoise, B., G. V. Latham, J. Daniel, J. Dupont, and A. K. Ibrahim, Seismic refraction studies in the New Hebrides and Tonga area, *U. N. ESCAP-CCOP/SOPAC Tech. Bull., 3*, 47-58, 1980.

Rait, G., F. Chanier, and D. W. Waters, Landward- and seaward-directed thrusting accompanying the onset of subduction beneath New Zealand, *Geology, 19*, 230-233, 1991.

Reyners, M., New Zealand seismicity 1964-87: An interpretation, *N. Z. J. Geol. Geophys., 32*, 307-315, 1989.

Ryan, H. F., and P. J. Coleman, Composite transform-convergent plate boundaries: Description and discussion, *Mar. Pet. Geol., 9*, 89-97, 1992.

Ryan, H. F., and D. W. Scholl, The evolution of the forearc structures along an oblique convergent margin, central Aleutian arc, *Tectonics*, *8*, 497-516, 1989.

Sandwell, D. T., and W. Smith, New global marine gravity map/grid based on stacked ERS-1, Geosat and Topex altimetry, *EOS, Trans. AGU*, *75(16)*, Spring Meet. Suppl., 321, 1994.

Schreurs, G., Experiments on strike-slip faulting and block rotation, *Geology*, *22*, 567-570, 1994.

Strong, C. P., Early Paleogene foraminifera from Matakoa Volcanic Group, *N. Z. J. Geol. Geophys.*, *23*, 267-272, 1980.

Strong, C. P., Late Cretaceous foraminifera from Hikurangi Plateau, New Zealand, *Mar. Geol.*, *119*, 1-5, 1994.

Sutherland, R., The Australia-Pacific boundary and Cenozoic plate motions in the Southwest Pacific: Some constraints from Geosat data, *Tectonics*, *14*, 819-831, 1995.

Taylor, B., Rifting and the volcanic-tectonic evolution of the Izu-Bonin-Mariana Arc, *Proc. Ocean Drill. Program, Sci. Results*, 126, 627-651, 1992.

Teyssier, C., B. Tikoff, and M. Markley, Oblique plate motion and continental tectonics, *Geology*, *23*, 447-450, 1995.

Vogt, P. R., Subduction and aseismic ridges, *Nature*, *241*, 189-191, 1973.

Vogt, P., A. Lowrie, D. R. Bracey, and R. N. Hey, Subduction of aseismic ocean ridges: Effects on shape, seismicity and other characteristics of consuming plate boundaries, *Spec. Pap., Geol. Soc. Am.*, *172*, 1976.

Von Huene, R., and R. Culotta, Tectonic erosion at the front of the Japan Trench convergent margin, *Tectonophysics*, *160*, 75-90, 1989.

Von Huene, R., and S. Lallemand, Tectonic erosion along the Japan and Peru convergent margins, *Geol. Soc. Am. Bull.*, *102*, 704-720, 1990.

Von Huene, R., and D. W. Scholl, Observations at convergent margins concerning sediment subduction, subduction erosion, and growth of continental crust, *Rev. Geophys.*, *29*, 279-316, 1991.

Walcott, R. I., Geodetic strain and the deformation history of the North Island of New Zealand during the late Cainozoic, *Philos. Trans. R. Soc. London*, Ser. *A*, *321*, 163-181, 1987.

Walcott, R. I., Paleomagnetically observed rotations along the Hikurangi margin of New Zealand, in *Paleomagnetic Rotations and Continental Deformation*, edited by C. Kissel, and C. Laj, pp. 459-471, Kluwer Acad., Norwell, Mass., 1989.

Wood, R., and B. Davy, The Hikurangi Plateau, *Mar. Geol.*, *153-173*, 1994.

Wright, I. C., Pre-spread rifting and heterogeneous volcanism in the southern Havre Through back-arc basin, *Mar. Geol.*, *113*, 179-200, 1993.

Wright, I. C., Nature and tectonic setting of the southern Kermadec submarine arc volcanoes: An overview, *Mar. Geol.*, *118*, 217-236, 1994.

J.-Y. Collot, Géosciences Azur, ORSTOM, B. P. 48, 06230, Villefranche sur mer, France. (e-mail: collot@ccrv.obs-vlfr.fr)

B. Davy, IGNS, P. O. Box 1320, Wellington, New Zealand. (e-mail: b.davy@gns.cri.nz)

(Received March 10, 1997; revised July 10, 1997;
accepted September 3, 1997.)

JOURNAL OF GEOPHYSICAL RESEARCH, VOL. 103, NO. B4, PAGES 7107–7110, APRIL 10, 1998

Correction to "Forearc structures and tectonic regimes at the oblique subduction zone between the Hikurangi Plateau and the southern Kermadec margin" by Jean-Yves Collot and Bryan Davy

In the paper "Forearc structures and tectonic regimes at the oblique subduction zone between the Hikurangi Plateau and the southern Kermadec margin" by Jean-Yves Collot and Bryan Davy (*Journal of Geophysical Research, 103*(B1), 623-650, 1998), all intermediate contours (25 m) disappeared in the three detailed bathymetric figures (Figures 4, 5, and 6), leaving only the 100-m contours, whereas the captions indicate that contours are 25 m. The 25-m contours are significant and very important for this study since they allow visualization of fine-grained morphologic features that are critical to our interpretation of an active margin being underthrust by a thick, buoyant oceanic plateau. Figures 4, 5, and 6 are reprinted here with all the details contained in the original figures (25-m contours).

(Received February 11, 1998.)

Paper number 98JB00871.
0148-0227/98/98JB-00871$09.00

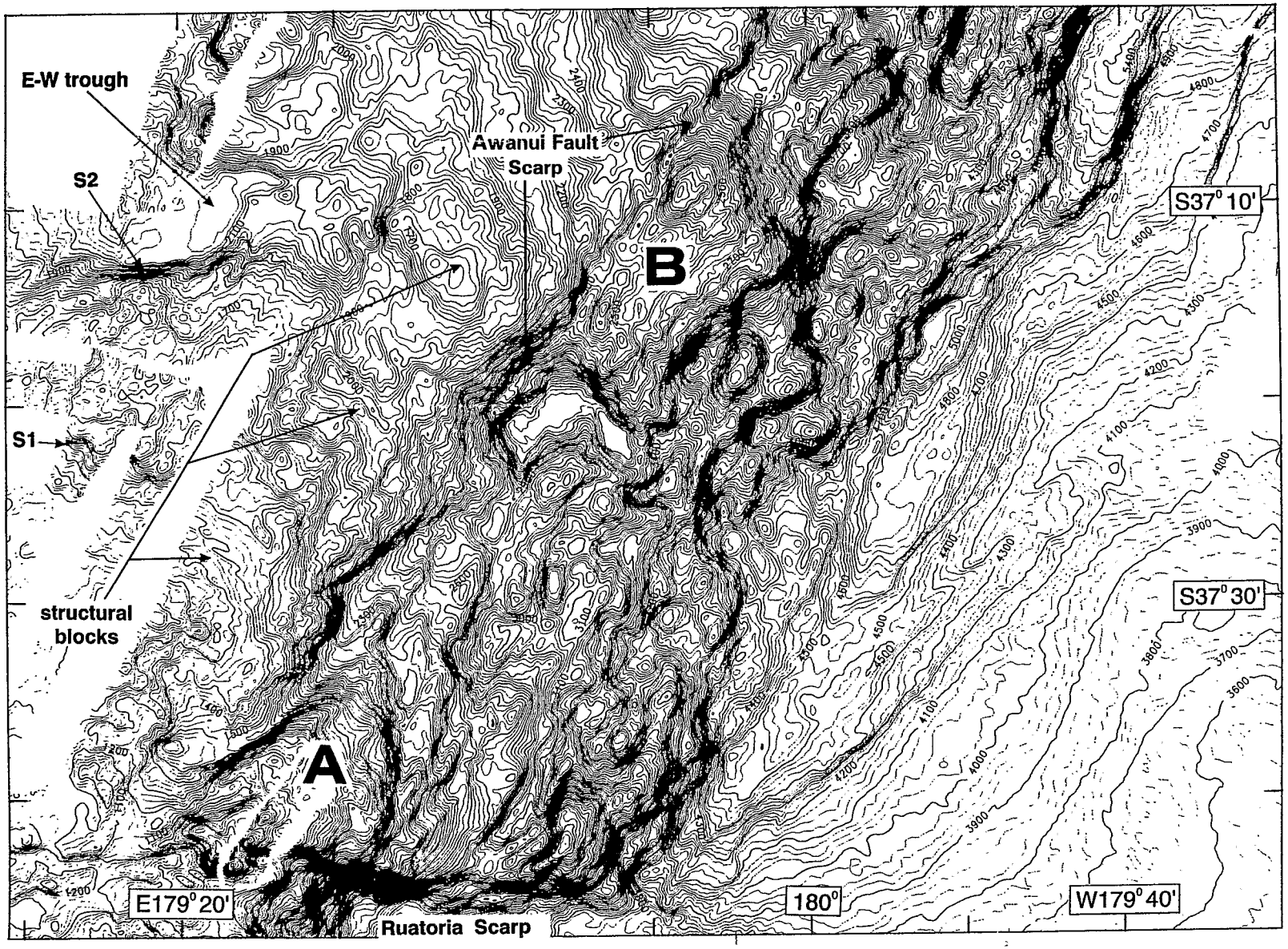

Figure 4. Multibeam bathymetric map of the southern part of the South Kermadec Trench; contours are 25 m. S1 and S2 are fault scarps, and A and B are structural blocks described in text. Location as shown in Figure 2.

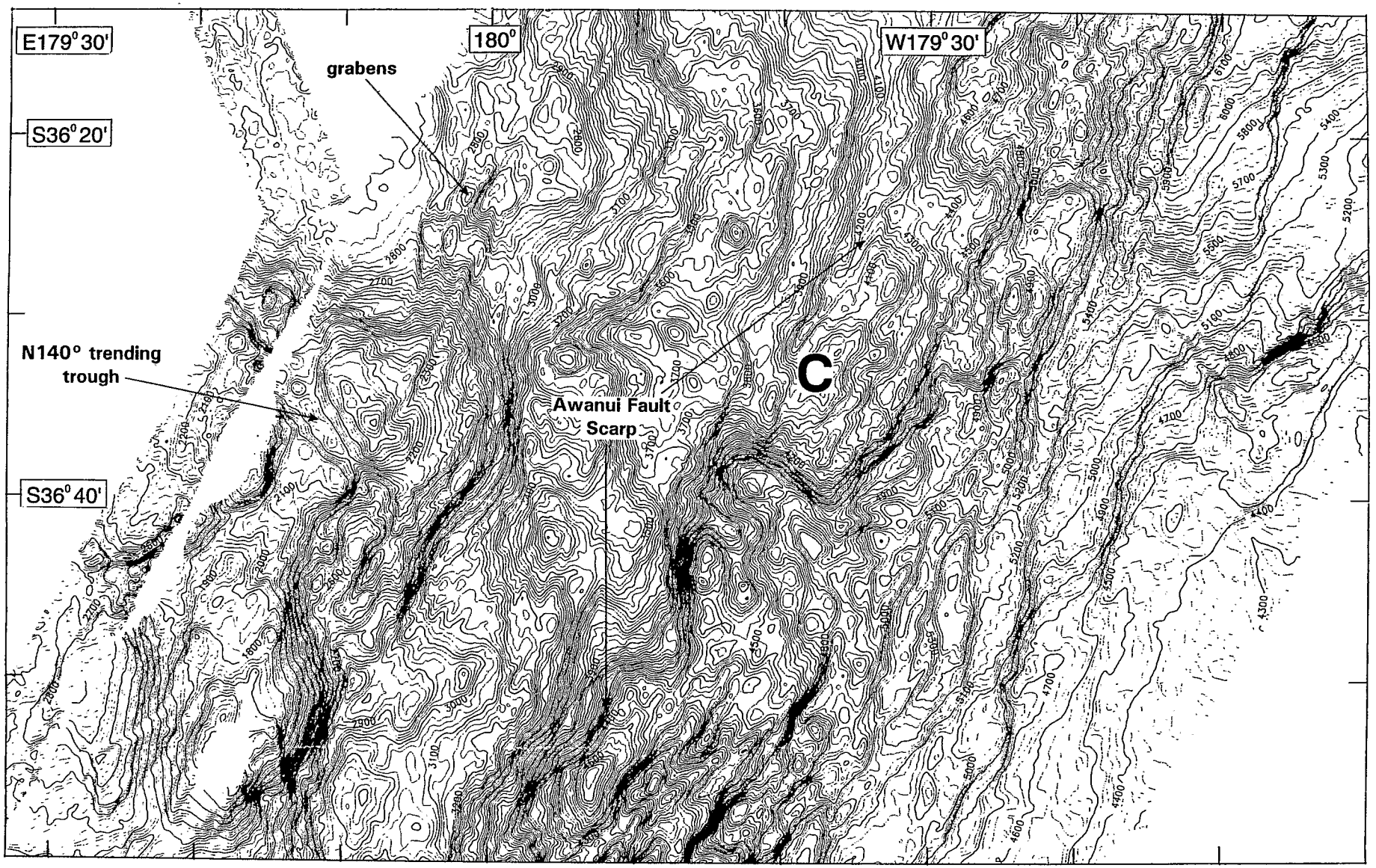

Figure 5. Multibeam bathymetric map of the central part of the South Kermadec Trench; contours are 25 m. Location as shown in Figure 2. C is structural block described in text.

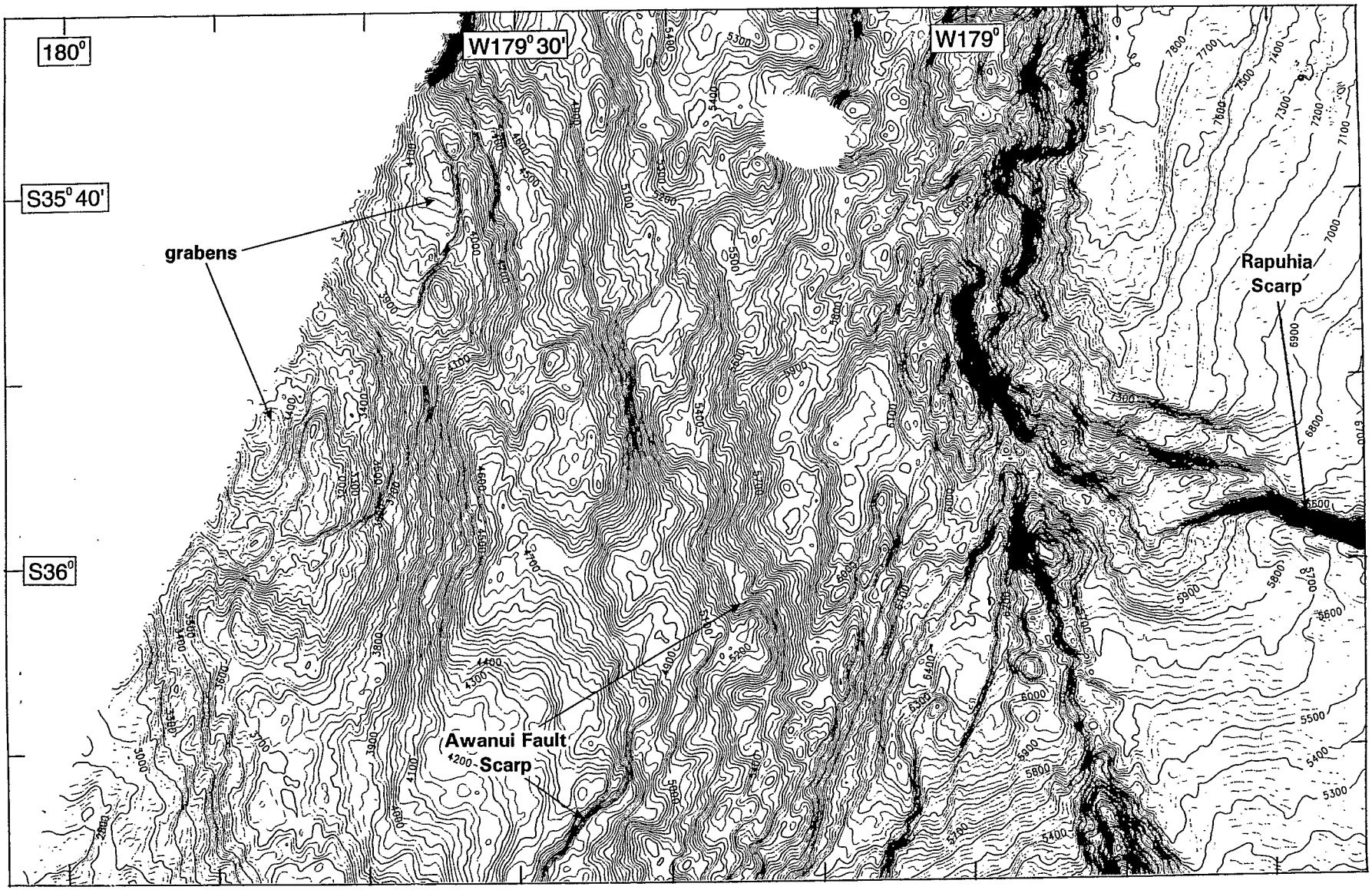

Figure 6. Multibeam bathymetric map of the northern part of the South Kermadec Trench; contours are 25 m. Location as shown in Figure 2.